Rechargeable Battery Circuit Modeling and Analysis of the Battery Characteristic in Charging and Discharging Processes

by

Dexinghui Kong

A Thesis Presented in Partial Fulfillment
of the Requirements for the Degree
Master of Science

Approved July 2012 by
Graduate Supervisory Committee:

Keith Holbert,Chair
Raja Ayyanar
George G. Karady

ARIZONA STATE UNVERSITY

August 2012

ABSTRACT

In this thesis, an issue is post at the beginning, that there is limited experience in connecting a battery analytical model with a battery circuit model. Then it describes the process of creating a new battery circuit model which is referred to as the kinetic battery model. During this process, a new general equation is derived. The original equation in the kinetic battery model is only valid at a constant current rate, while the new equation can be used for not only constant current but also linear or nonlinear current. Following the new equation, a circuit representation is built based on the kinetic battery model. Then, by matching the two sets of differential equations of the two models together, the ability to connect the analytical model with the battery circuit model is found. To verify the new battery circuit model is built correctly, the new circuit model is implemented into PSpice simulation software to test the charging performance with constant current, and Matlab/Simulink is also employed to simulate a realistic battery charging process with two-stage charging method. The results have shown the new circuit model is available to be used in realistic scenarios. And because the kinetic battery model can describe different types of rechargeable batteries, the new circuit model is also capable to be used for various battery types.

ACKNOWLEDGMENTS

My profound gratitude first goes to Professor Keith Holbert, my supervisor, who is busy for teaching job but still shared his precious time for our discussion of the thesis details. His expertise and insight have been influential in performing this research work. His teaching and work ethic are an inspiration. He is always patient to look at my thesis sentence by sentence, to help me find out the best way to express my work and correct mistakes. I would also like to thank the members of my supervisory committee, Prof. Raja Ayyanar and George G. Karady for their support.

I want to thank my parents, they always stand on my side to support me. I could not come to U.S to study without their help. They are not only my parents but also my best friends.

My sincere thanks also go to my lab mates; it has been so joyful to work with them during the past two years. I was particularly grateful Hui Zhang for his kindness and great help. I am also obliged to my wife in China as well as my friends for their support and encouragement. Without you, I could not have gone that far.

TABLE OF CONTENTS

Page

Page

LIST OF TABLES

Table Page

LIST OF FIGURES

Figure Page

Figure Page

NOMENCLATURE

EV	Electric Vehicle
IEEE	Institute of Electrical and Electronics Engineers
q_1	Available charge of the battery
q_2	Bound charge
U	Electrode potential
i_0	Exchange current density
η	Polarization or overvoltage
R	Molar gas constant ($8.3143 J*mole^{-1}*K^{-1}$)
α_c	Cathodic charge transfer coefficient which equals 0.5
α_a	Anodic charge transfer coefficient which equals 0.5
δ_{sep}	Thickness of the separator
δ	The thickness of negative electrode
A	Electrode plate area
σ	Active material reference conductivity
σ^{eff}	Effective conductivity of the solid matrix
D^{eff}_e	Effective diffusion coefficient
t^0_+	Transference number of Li-ions with respect to the velocity of the solvent
ε_e	Electrolyte phase volume fraction
c_e	Electrolyte phase lithium concentration
j^{Li}	Volumetric rate of electrochemical reaction at the particle surface

N_j	Flux of species j
Φ_e	Electrolyte potential
Φ_s	Solid potential
ε_s	Active material volume fraction
ε_f	Conductive filler volume fraction
c_j	Concentration of species j in mole*cm^{-3}
D	Diffusion coefficient in cm^2*s^{-1}
t	Transference number
z_j	Valence number
ξ	Diffusion direction in cm
F	Faraday constant which is 96487 C/mol
a_s	Specific interfacial surface area
h_1	The depth of the capacity in Tank 1
h_2	The depth of the capacity in Tank 2

CHAPTER 1

INTRODUCTION

1.1 Rechargeable Battery History

In the U.S., about 15.4 million barrels of oil are used each day, and 2/3 of these are refined into automobile fuel [1]. There is a clear economic and political incentive for the development of electric vehicles, considering the fast consumption and high price of oil and gasoline. Due to multiple reasons, rechargeable batteries were developed and are widely used in the world from a small cell phone battery to a large energy storage battery. The rechargeable batteries have had a history for over 150 years since the first one was invented by Gaston Plante in 1859 [2]. Rechargeable batteries are also known as secondary cells because their electrochemical reactions are electrically reversible. Battery technology continues to develop, because of advancements in chemical materials and electrochemistry. Different kinds of secondary batteries were invented by using various materials, such as lead-acid, nickel-iron, nickel-hydrogen and lithium-ion batteries. These batteries have their own special characteristic.

For example, the lead acid battery, which has an over 140 years of development, can deliver very high currents. This makes it a good choice to be a backup power source for high load facilities. The lead acid battery also can tolerate overcharge. And it has low internal impedance, which means the battery will have a higher efficiency when delivering power to loads. The lead acid battery also has its own shortcomings. For example, the battery is very heavy and bulky, so it has been replaced by other rechargeable battery in portable device. Lead acid battery

also has a short cycle life of 300 to 500 cycles, and this will raise the cost for battery source facilities. In the meantime, it is not suitable for fast charging too.

Compared with the lead-acid battery, the lithium-ion battery is a new rechargeable battery and developing very fast in recent years. The lithium-ion battery can be charged anytime with no memory effect, which makes it widely used in facilities with high operation frequency, such as cell phones and laptops. Lithium-ion batteries also have the ability to provide higher open circuit voltage and lower self-discharge rate than other secondary batteries, such as lead-acid, nickel-metal hydride and nickel-cadmium. With these advantages, Li-ion can also be chosen as an energy supply for electrical cars. However it is not perfect either, since the lithium-ion batteries have higher internal resistance than other types of batteries, this will increase losses, and the cell life is decreased over time due to high charge and discharge level [3].

1.2 The Development of Rechargeable Batteries

In recent years, a number of researchers have begun to investigate the characteristics of rechargeable batteries. They built different types of battery models for various materials. Some researchers study the basic theories of batteries, and built an analytical model based on theoretical analysis. A low-level detailed electrochemical model based on concentrated-solution theory was reported in [4]; this electrochemical model is used for lithium-ion battery simulation. Other researchers use experimental measurement to obtain data and built a circuit model from simulator software. Based on analysis of the traditional rechargeable battery

equivalent circuit models, the RC, Thevenin and Partnership for a New Generation of Vehicles (PNGV) models are developed [5].

In this thesis, the analytical models and circuit models for rechargeable batteries are studied, and the analytical model characteristics are simulated using Matlab. A relationship between the analytical models and circuit models is found by relating the analytical model results with circuit model parameter equations. Circuit model parameters are suppose to be estimated by comparing the average cell voltage and the temperature for different charge and discharge rates. There have been some works that applied the circuit analog approach for lead acid, nickel metal hydride, Li-ion batteries and activated-carbon capacitors in a proper way to predict the state of charge (SOC), state of health (SOH) and power capability [6]. Reference [7] presented a one-dimension electrochemical model of a lithium-ion battery. In this model, the researcher analyzes the concentration of lithium ions, and finds the relationship between the ion concentration with battery voltage and state of charge. Electrochemistry analytical models are accurate but they usually require long simulation times in practice. Consequently, more efficient battery models have been proposed in recent years.

Another analytical model which can be used for computing battery lifetimes is the kinetic battery model of Manwell and McGowan [8]. In their model the battery charge is distributed over two wells: the available-charge well and the bound-charge well. When a load is applied to the battery, the available charge reduces while the capacity of the charge well is increased. When the load is removed,

charge flows from the bound-charge well to the available-charge well until both well capacities are equal again [9], this is also called recovery effect.

The kinetic battery model is simple and easy to understand, but it is not available to show the battery I-V relationship and is not able to show the state of charge of the battery. Besides, the kinetic battery model assumes the current flow is constant which cannot satisfy a realistic scenario. In order to solve this problem and find a relationship between a battery analytical model and the battery circuit model, a new equation to describe the kinetic battery model has been derived, and a new circuit model is also built based on the kinetic battery model. According to matching the two sets of equations for the analytical model and the circuit model together, the relationship between the two types of battery models has been found.

CHAPTER 2

LITERATURE REVIEW

2.1 Background Study

In recent years, the growth of electric driven automobiles has tremendously increased. Up to now, most of the cars are still relied on gasoline and diesel. In the U.S., 2/3 of the barrels of oil are refined into automobile fuel, and automobile emissions are also known to add a significant amount of pollutants to the air each year. Petroleum is presently the only resource to extract gasoline and diesel, and it has been announced by EU Energy Policy that reserves can only supply the consumption for no more than 47 years. It will bring big trouble to the modern transportation system if people do not find an effective solution before petroleum runs out. To solve this problem, electric vehicles have received significant interest from multiple countries, and they invest a large sum of money to support the development of electric vehicles. However, some restrictions on technology, especially on rechargeable batteries, make it hard to develop a pure electric vehicle. The main problem is that the driving range of pure electric vehicles is a lot shorter than gasoline cars. For example, Nissan produced a pure electric vehicle called "Leaf", which can go 73 miles with one full charge of the battery. Even though the car has zero emissions, but the 73 miles driving range means people have to charge the car every day, and probably it can only be driven in the city.

The crisis awareness of gasoline cars, and the attractiveness of electric vehicles make lots of automobile companies start to develop hybrid vehicle. Hybrid vehicles have two power systems: electromotor and combustion engine. When the

car is starting, climbing, accelerating and driving in local, the electromotor will work to release the combustion engine and reduce pollution. When the car is driving on highway or in normal speed, the combustion engine will take place of the electromotor. On the other hand, the car battery will be charged while the driver applies the brake or downhill. For example, Toyota produced a hybrid vehicle called “Prius” which is the most popular hybrid vehicle selling in the U.S. The car is using a sealed 38-module nickel metal hydride (NiMH) battery pack providing 273.6 volts, 6.5 Ah capacity and weighing 53.3 kg [10].

All of these electric vehicles need a power source, the rechargeable battery. It is important to know the trends in vehicle energy storage, this will allow better prediction and modeling of the system load under vehicle charging conditions.

The charging process and method are very important for rechargeable batteries, to maintain a proper charging method can help to extend the battery life. However, different rechargeable batteries have diverse chemical components with decidedly unique characteristics and behaviors, and they will be used in various applications as well. For example, the lithium-ion battery and the lithium-polymer battery are smaller, lighter and have bigger capacity than other rechargeable batteries, so they are widely used in cameras, laptops, mobile phones and other portable electric products. While the lead-acid batteries have little internal resistance and stable performance, and are widely used in automobiles and motorcycles. Thus the charging process should be changed for different type of batteries to protect the battery during charging and make sure the battery is fully charged.

In order to establish consensus regarding the methods and requirements of electric vehicle charging, three charging levels were defined by the Electric Power Research Institute and codified in the National Electric Code (NEC) [11].

The Level 1 method uses a standard 120 VAC, 15 amp (12 amp useable) or 20 amp (16 amp useable) branch circuit that is the lowest common voltage level found in both residential and commercial buildings in the United States. Level 1 only provides a small amount of power, and can result in a long charge time, so it was only intended to be an entry level voltage and it is not the ultimate charging solution. An advantage of charging at Level 1 is the availability of 120 VAC outlets in an emergency situation, even though that might take several hours to get charged.

The Level 2 method is described as the "primary" method for a battery electric vehicle charger for both private and public facilities at a 240 VAC, single-phase, 40 amp branch circuit. The Level 2 method use a special inductive equipment to provide a higher level of safety required by the NEC. The inductive system has no metal-to-metal contact and inductively transfer energy to the vehicle. Additionally, due to the small battery size of the electric vehicle, Level 2 charging in many instances will be limited to 15 A, which means it will provide a maximum charge power of 3.3 kW.

The Level 3 method, which is also called "Fast Charging", is for commercial and public applications and is intended to be used similar to a gasoline station. Level 3 uses a charge system serviced by a 480 VAC, three-phase circuit. If the

battery electric vehicles (varied from 60 to 150 kW) achieve a 50% charge in 10 to 15 minutes, this is considered to meet the intent of Level 3 charging [11].

The three levels of charging methods have their own advantages and disadvantages, and they have been used in different way. For example, Level 1 is normally used for the small power facilities charger, Level 2 is used for an electric vehicle or hybrid vehicle charger, and Level 3 is usually used for large battery energy storage systems or battery backup systems.

Nowadays, lead-acid batteries are still widely used in gasoline cars and hybrid cars, however the energy density of the lead-acid battery (50 Wh/kg [12]) seems to be a little bit low for battery electrical cars. Since the driving range for the battery electrical cars is really limited, so the heavier the car is, means the shorter distance the car will go. It is necessary to have a lighter and bigger capacity battery for the electrical cars. The lithium-ion liquid electrolyte batteries are now well established, and the energy densities are around 150 Wh/kg. While in the future, there are prospects of increases in the energy density to perhaps 200-250 Wh/kg by using new cathode materials and light weight construction, such as lithium nickel cobalt oxide [13]. High power cells make the future batteries possible to find new uses, for example, in military applications to support electronic devices as a power source in remote locations. And some new materials could reduce the cost, which might make lithium rechargeable batteries more economical for electric vehicles.

It is necessary to analyze the charging and discharging characteristic of re-chargeable batteries to develop a better charge method. The Li-ion batteries have higher voltage, tighter voltage tolerance and usually it is not required to have trickle or float charge for lithium batteries when full charge is reached. The charge time of all Li-ion batteries is about 3 hours, when charged at a 1 C/s initial current, and the battery remains cool during charge. This is the first stage which is charging the battery with constant current. While it reaches the upper cell voltage, the current will drop and level off at about 3 percent of the nominal charge current. Then it charges the battery with a constant voltage until the battery is fully charged. The charging stages of a Li-ion battery are shown in Fig. 1. Fig. 2 shows how the battery capacity changes under different stages.

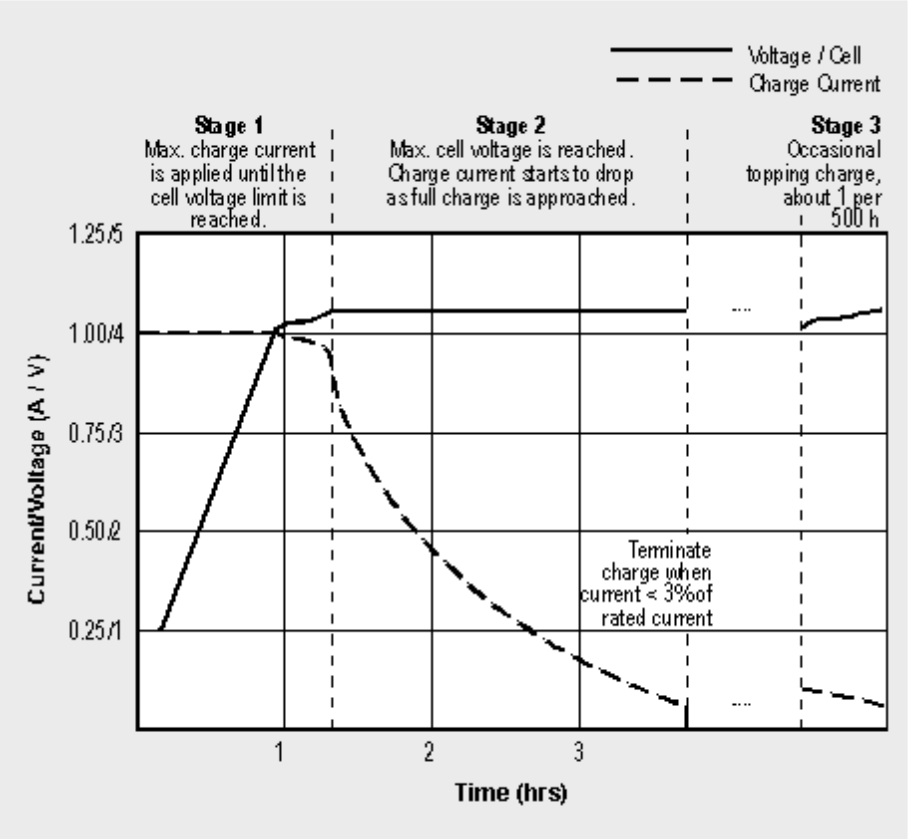

Fig. 1. Charging stages of a Li-ion battery [14].

There are differences for lithium-ion batteries compared with other battery types, that increasing the charge current on a lithium-ion charger does not shorten the charge time by much. It is true that the battery peak voltage is reached quicker with higher current, but the Stage 2 will take longer. Usually there is no trickle charge applied on lithium-ion batteries because they are unable to absorb over-charge. A trickle charge could cause plating of metallic lithium on the electrode and leads to unstable condition to the cell [14].

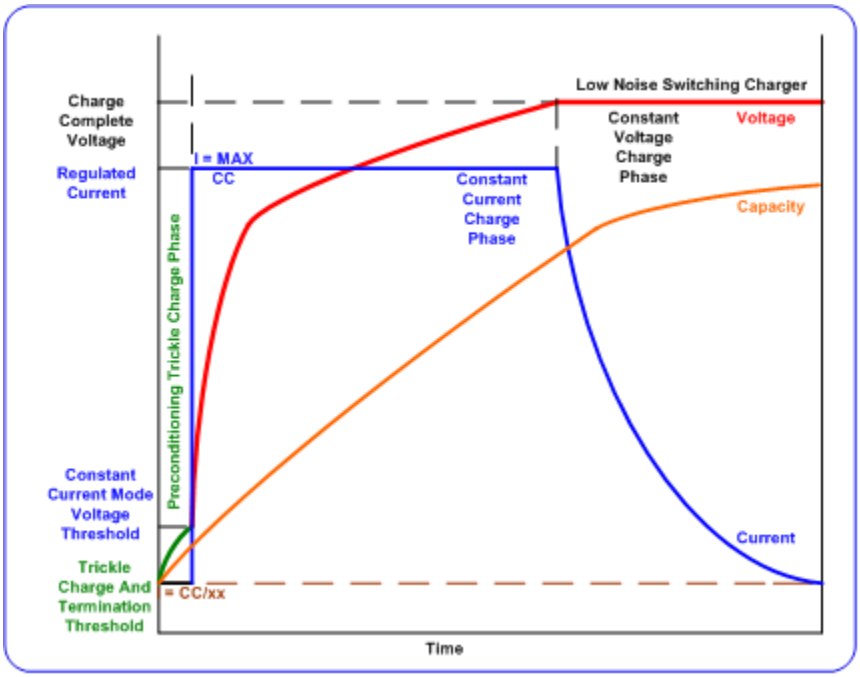

Figure 2. Battery capacity performance under different stages [15].

2.2 Model Study

The demand for energy storage sources of high energy density has been growing quickly recently as a result of stimulation of portable personal electronics and energy storage system, such as automobile starters, motorized wheelchairs, cell phones, and uninterruptible power supplies. Wide use in the world leads more and more researchers trying to improve the technology to reduce cost and weight, and increase lifetime.

In this section, two analytical battery models are studied. One of the analytical battery models is based on diffusion of the ions and another is the kinetic battery model. The diffusion model analyzes the ion diffusion and migration in both electrodes and electrolyte, then calculates the battery internal resistances and capacitances through the relationship between ions concentration and battery voltage. While the kinetic battery model is simpler than the diffusion model by providing a more intuitive and general battery model, and instead of finding the battery voltage characteristic, the primary concern of the kinetic battery model is power flow, then, the internal resistance is calculated with a controlled power flow. At last the battery capacity performance will be shown by the equations in the kinetic battery model. In the end of this section, the circuit models are studied. The Thevenin equivalent circuit is widely used to describe a battery model, because of its low error rate compared with the other two circuit models (RC and the Partnership for a New Generation of Vehicles circuit model are mentioned in this section).

2.2.1 Electrochemical Diffusion Model

An analytical battery model based on the diffusion of the ions in the electrolyte has been presented in references [7], [16]. Fig. 3 shows the lithium-ion battery consists of three parts: a positive electrode, a negative electrode and a separator.

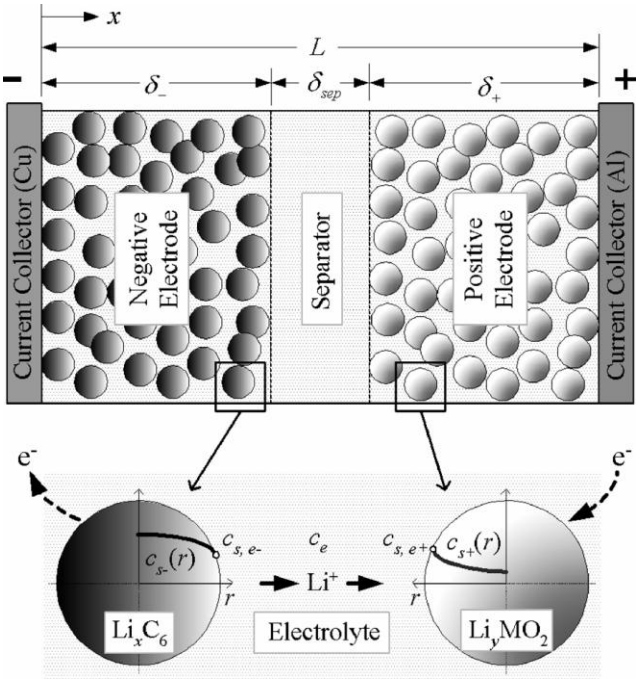

Figure 3. Schematic of a lithium-ion cell [7].

The model describes the evolution of the concentration of the electro-active species in the electrolyte to predict the battery lifetime under a given discharge current or load. The voltage characteristic is then obtained according to the inter relationship between concentration and battery voltage. This model is detailed in the remainder of this subsection in order to provide the reader with an appreciation of the complexities of such a depiction.

Diffusion and Migration: Fick's second law is applied as a basic function

$$N_j = \frac{i_j}{n \cdot F} = -D_j \frac{\partial c_j}{\partial \xi} + \frac{i \cdot t_j}{z_j \cdot F} \tag{1}$$

With N_j : flux of species *j* in mole*cm^{-2}; n is the number of particles. $\frac{i_j}{n \cdot F}$: current equivalent; c_j : concentration of species *j* in mole*cm^{-3}; $\frac{\partial c_j}{\partial \xi}$: concentration gradient in mole*cm^{-4}; *D*: diffusion coefficient in cm^2*s^{-1}; *t*: transference number; z_j : valence number, ξ : diffusion direction in cm. *F* is Faraday constant which is 96487 C/mol.

The first addend also can be replaced by:

$$D_j \frac{\partial c_j}{\partial \xi} = -\frac{j^{Li}}{a_s \cdot F} \tag{2}$$

Where a_s is the specific interfacial surface area, and can be calculated as: $a_s = 3\varepsilon_s / R_s$, R_s is the spherical radius. ε_s is the active material particles occupying electrode volume fraction, it equals 0.58 for the negative electrode, and 0.5 for the positive electrode. j^{Li} is the volumetric rate of electrochemical reaction at the particle surface (with j^{Li} larger than zero indicating ion discharge).

In the battery electrolyte, the ion diffusion process yields,

$$\frac{\partial(\varepsilon_e c_e)}{\partial t} = \frac{\partial}{\partial x}(D_e^{eff} \frac{\partial}{\partial x} c_e) + \frac{1 - t_+^0}{F} j^{Li} \tag{3}$$

The zero flux boundary condition at the current collectors can be denoted as

$$\left.\frac{\partial c_e}{\partial x}\right|_{x=0} = \left.\frac{\partial c_e}{\partial x}\right|_{x=L} = 0 \tag{4}$$

Where $c_e(x, t)$ is the electrolyte phase lithium concentration, ε_e is the electrolyte phase volume fraction, t^0_+ is the transference number of lithium ions with respect to the velocity of the solvent, and here it equals 0.363. The effective diffusion coefficient D_e^{eff} can be calculated from a reference coefficient using the Bruggeman relation:

$$D_e^{eff} = D_e \varepsilon_e^p \tag{5}$$

For the electrode, charge conservation can be described by Ohm's law,

$$\frac{\partial}{\partial x}(\sigma^{eff} \frac{\partial}{\partial x}\phi_s) - j^{Li} = 0 \tag{6}$$

With boundary conditions at the current collectors as,

$$-\sigma_-^{eff} \left.\frac{\partial \phi_s}{\partial x}\right|_{x=0} = \sigma_+^{eff} \left.\frac{\partial \phi_s}{\partial x}\right|_{x=L} = \frac{I}{A} \tag{7}$$

and zero electronic current at the separator,

$$\left.\frac{\partial \phi_s}{\partial x}\right|_{x=\delta_-} = \left.\frac{\partial \phi_s}{\partial x}\right|_{x=\delta_- + \delta_{sep}} = 0 \tag{8}$$

Where ϕ_s(x,t) and σ^{eff} are the potential and effective conductivity of the solid matrix, respectively. σ^{eff} can be calculated by the active material reference conductivity σ as $\sigma^{eff}= \sigma\varepsilon_s$. In Equation (7), A is the electrode plate area. δ denotes the thickness of negative electrode, while δ_{sep} represent the thickness of the separator.

The volumetric rate of electrochemical reaction at the particle surface, j^{Li}, can be calculated as follows:

$$j^{Li} = a_s \cdot i_0 \left\{ \exp\left[\frac{\alpha_a \cdot F}{RT} \eta \right] - \exp\left[-\frac{\alpha_c \cdot F}{RT} \eta \right] \right\} \tag{9}$$

Where α_a and α_c are the anodic and cathodic charge transfer coefficients, respectively, and are 0.5. The exchange current density, i_0, characterizes the dynamic equilibrium. R is the molar gas constant (8.3143 J*mole^{-1}*K^{-1}). T is absolute temperature.

$$\eta = U - U^O \tag{10}$$

η is the polarization or overvoltage, and can be found using handbooks, such as [17]. When η is positive, it means overvoltage, when η is negative, it means reduced voltage.

In electrode reactions, *n*F*U* is the driving force, and the corresponding relation is:

$$i = k^{'} \cdot c_j \cdot \exp\left(\frac{n \cdot F}{RT} U \right) \tag{11}$$

Where $k^{'}$ includes the equivalence factor *n*F* between mass transport and current *I*; *U* is the electrode potential; c_j is the concentration of the reacting substance that releases or absorbs electrons. So we can transform equation:

$$i = k_{+} \cdot c_{red} \cdot \exp\left(\frac{\alpha \cdot n \cdot F}{R \cdot T} U\right) - k_{-} \cdot c_{ox} \cdot \exp\left(-\frac{(1-\alpha) \cdot n \cdot F}{R \cdot T} U\right) \tag{12}$$

into

$$i = i_0 \left[\exp\left(\frac{\alpha \cdot n \cdot F}{RT} \eta\right) - \exp\left(-\frac{(1-\alpha) \cdot n \cdot F}{RT} \eta\right)\right] \tag{13}$$

The electrochemical diffusion model is the most accurate analytical battery model, but as can be seen from the partial differential equations, this model is complicated to build a circuit model. Then, in order to find a proper analytical model and build a related circuit model, the Kinetic battery model is presented in following section.

2.2.2 Kinetic Battery Model

In the kinetic battery model [8], the voltage source is modeled as two tanks separated by a conductance. One tank represents the battery capacity that is available to be used by the load at any time. The conductance corresponds to the rate constant of an electrochemical diffusion process which makes the bound charge become available. While the second tank shows the capacity of charging and it is assumed to connect to the electric grid. Fig. 4 shows the model. Each tank has

unit depth, but different widths, corresponding to different volumes. The surface area of tank 1 is *c*, and the second tank surface area is 1-*c*. Since the width of the two tanks added together equals 1, that makes the combined tank surface area unity. The combined volume of the two tanks is q_{max}, which is the maximum battery capacity. Since the energy level height is *h* when both tanks are full, *h* equals q_{max} and reaches its maximum value. The fixed conductance between those two tanks is *k'*. The load current, *I*, is considered as constant for a specific discharge time.

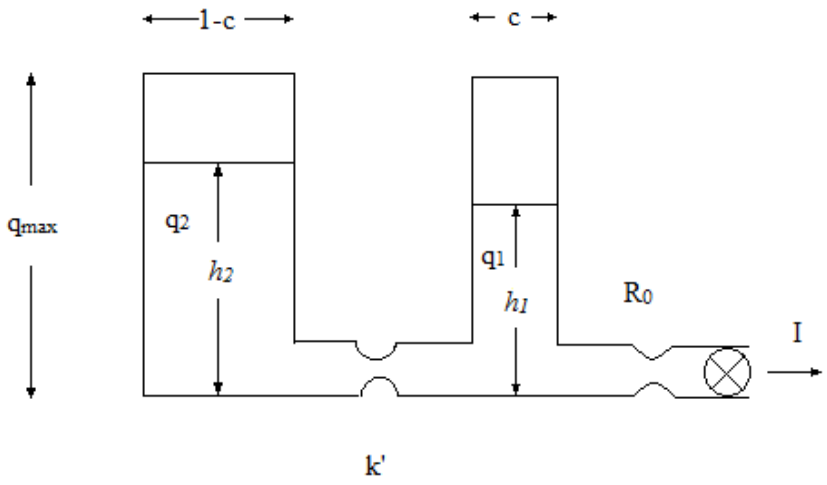

Figure 4. Kinetic battery model adaption [8].

The equations describing the battery are:

$$\frac{dq_1}{dt} = -I - k'(h_1 - h_2) \qquad (0 < q_1 \leq cq_{max}) \qquad (14)$$

$$\frac{dq_2}{dt} = k'(h_1 - h_2) \qquad (0 < q_2 \leq (1-c)q_{max}) \qquad (15)$$

Where q_1 is available charge of the battery, q_2 is bound charge, h_1, h_2 is the depth of the capacity in each tank, which can be calculated as the ratio of tank capacity and surface area:

$$h_1 = \frac{q_1}{c} \qquad (0 < q_1 \leq cq_{max}) \qquad (16)$$

$$h_2 = \frac{q_2}{(1-c)} \qquad (0 < q_2 \leq (1-c)q_{max}) \qquad (17)$$

For mathematical simplicity, a new rate constant k is defined as

$$k = \frac{k'}{c(1-c)} \qquad (18)$$

Then substituting Equations (16), (17), and (18) into Equations (14) and (15), the new version of equations (14) and (15) can be solved by using the Laplace transform method and written as

$$Q_1(s) = \frac{q_{1,0}}{s+k} - \frac{I}{s^2+sk} + \frac{kcq_0}{s^2+sk} - \frac{kcI}{s^3+s^2k}$$

$$Q_2(s) = \frac{q_{2,0}}{s+k} - \frac{I}{s^2+sk} + \frac{k(1-c)q_0}{s^2+sk} - \frac{k(1-c)I}{s^3+s^2k}$$

$$q_1 = q_{1,0}e^{-kt} - \frac{(q_0kc-I)(1-e^{-kt})}{k} - \frac{Ic(kt-1+e^{-kt})}{k} \qquad (19)$$

$$q_2 = q_{2,0}e^{-kt} - q_0(1-c)(1-e^{-kt}) - \frac{I(1-c)(kt-1+e^{-kt})}{k} \qquad (20)$$

Where $q_{1,0}$ and $q_{2,0}$ are initial conditions for the two tanks, and q_0 is the combined value of those two initial values, i.e., $q_0 = q_{1,0} + q_{2,0}$.

In the kinetic battery model, the model can be used in two ways. It depends on whether the voltage is to be considered explicitly or not. Here we make an assumption that the voltage variation with state of charge is not of concern. Thus there are three constants that need to be determined: q_{max}, the maximum capacity of the battery; c, the fraction of capacity that may hold available charge; and k, the rate constant. They can be calculated with battery capacity data provided by manufacturers. After those three constants are determined, the internal resistance R_0 will be solved.

Here a new parameter $F_{t1,t2}$ is defined, it is a ratio of different capacities for various discharge rates.

$$F_{T_1,T_2} = \frac{q_{t=T_1}}{q_{t=T_2}} \tag{21}$$

Where $q_{t=T}$ is the discharge capacity at a certain total discharge time, $t=T$ and T_1 and T_2 denote two different battery discharge times.

To find the constants c and k, it is necessary to assume that the battery is initially full, so the ratio of tank capacities is same as the ratio of widths. Then Equation (19) can be rewritten as

$$q_1 = q_{\max} c - \frac{I(1-e^{-kT})(1-c)}{k} - Ict \tag{22}$$

Where I is the discharge current.

The discharge current to empty the battery in time T, $I_{t=T}$, can be calculated by setting $q_1 = 0$ in Equation (22).

$$I_{t=T} = \frac{q_{\max} ck}{(1-e^{-kT})(1-c) + kcT} \tag{23}$$

Recognizing that $q_{t=T} = I_{t=T} * T$, Equation (21) becomes

$$F_{T1,T2} = \frac{\dfrac{T_1 q_{\max} ck}{(1-e^{-kT_1})(1-c) + kcT_1}}{\dfrac{T_2 q_{\max} ck}{(1-e^{-kT_2})(1-c) + kcT_2}} \tag{24}$$

Rearranging Equation (24), the constant 'c' can be calculated as

$$c = \frac{F_{T_1,T_2}(1-e^{-kT_1})T_2 - (1-e^{-kT_2})T_1}{F_{T_1,T_2}(1-e^{-kT_1})T_2 - (1-e^{-kT_2})T_1 - kF_{T_1,T_2}T_1T_2 + kT_1T_2} \tag{25}$$

Given any two F_{T_1,T_2} values, it is possible to calculate the constants k and c. Then, substitute the two constants into Equations (22) and (23) to acquire the expressions for battery capacity and discharge current.

2.2.3 Battery Circuit Models

Battery circuit models are developed by using electrical components to describe the battery dynamic characteristics and operation principles. Comparing with the analytical models, circuit models have their own advantages. Circuit models are easy to understand, and can be implemented into computer simulation tools. As long as the electronic component values are known, the simulation software will show the battery characteristic clearly. So the battery circuit model is very important to analyzing the performance of the battery.

For the battery circuit models, usually, an ideal voltage source or a large capacitor is selected to be the open circuit voltage (OCV) [5], and the remaining components of the circuit simulate the battery internal resistances and dynamic effects. In this section, three battery equivalent circuit models (the RC, Thevenin and PNGV) that have been mentioned before are studied.

The RC model, shown in Fig. 5, consists of two capacitors (C_c, C_b) and three resistors (R_t, R_e, R_c). The capacitor C_c usually represents the battery surface effects and has a small capacitance, and it is thus termed the surface capacitor. The capacitor C_b has a large capacitance and here represents the power source of the battery; it is called the bulk capacitor. The battery state of charge can be determined by the voltage across the bulk capacitor. Resistors R_t, R_e, R_c are named terminal resistor, end resistor and capacitor resistor, respectively [18]. U_b and U_c are the voltages across C_b and C_c, respectively. The electrical behavior of the circuit can be expressed by Equations (26) and (27) [5].

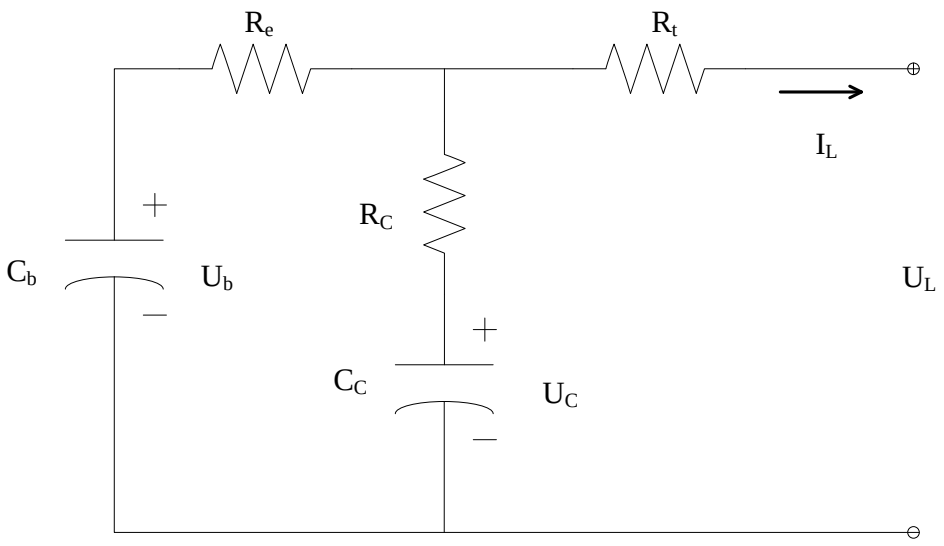

Figure 5, Schematic diagram of the RC battery model [5].

$$\begin{bmatrix} U_b \\ U_c \end{bmatrix} = \begin{bmatrix} \frac{-1}{C_b(R_e+R_c)} & \frac{1}{C_b(R_e+R_c)} \\ \frac{1}{C_b(R_e+R_c)} & \frac{-1}{C_b(R_e+R_c)} \end{bmatrix} \begin{bmatrix} U_b \\ U_c \end{bmatrix} + \begin{bmatrix} \frac{-R_c}{C_b(R_e+R_c)} \\ \frac{-R_e}{C_b(R_e+R_c)} \end{bmatrix} \begin{bmatrix} I_L \end{bmatrix} \tag{26}$$

$$\begin{bmatrix} U_L \end{bmatrix} = \begin{bmatrix} \frac{R_c}{(R_e+R_c)} & \frac{R_e}{(R_e+R_c)} \end{bmatrix} \begin{bmatrix} U_b \\ U_c \end{bmatrix} + \begin{bmatrix} -R_t - \frac{R_e R_c}{(R_e+R_c)} \end{bmatrix} \begin{bmatrix} I_L \end{bmatrix} \tag{27}$$

The Thevenin model is shown in Fig. 6. The circuit describes the battery dynamic characteristics with a parallel RC connected in series with R_o and an open-circuit voltage source U_{oc}. The internal resistances include the ohmic resistance R_o and the polarization resistance R_{Th}. The equivalent capacitance C_{Th} is used to describe the transient response during charging and discharging. U_{Th} is the

voltage across C_{Th}. I_{Th} is the outflow current of C_{Th}. The electrical behavior of the Thevenin model can be expressed by Equation (28)

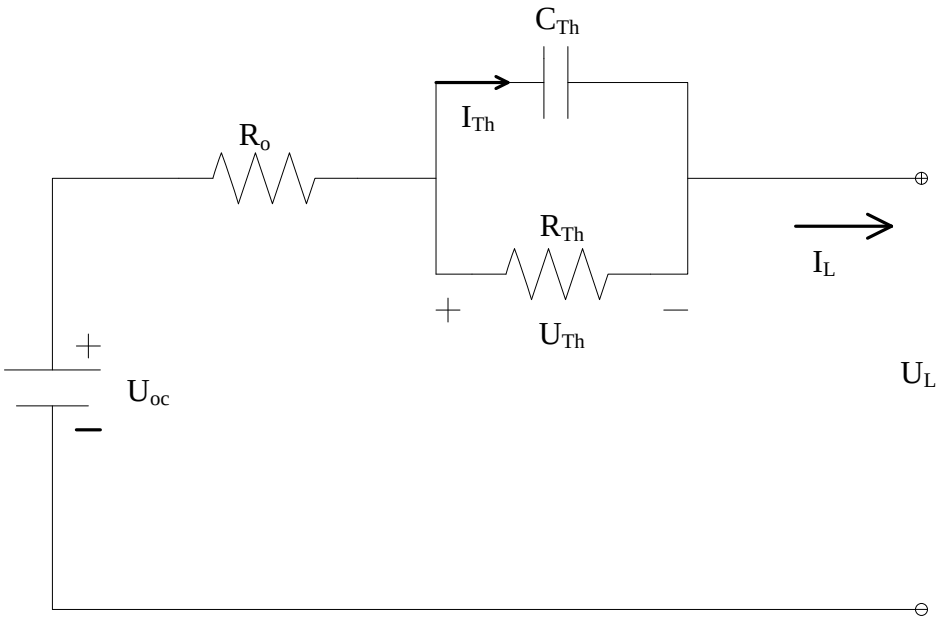

Figure 6. Schematic diagram for the Thevenin battery model [5].

$$\begin{cases} U_{Th} = -\dfrac{U_{Th}}{R_{Th}C_{Th}} + \dfrac{I_L}{C_{Th}} \\ U_L = U_{oc} - U_{Th} - I_L R_o \end{cases} \tag{28}$$

The PNGV model, as shown in Figure 7, can be obtained by adding a capacitor $1/U'_{oc}$ in series with the Thevenin model to describe the changing of open circuit voltage generated in the time accumulation of load current. U_d and U_{PN} are the voltage across $1/U'_{oc}$ and C_{PN} respectively. I_{PN} is the outflow current of C_{PN} [19]. The electrical behavior of the PNGV model can be expressed by Equation (29):

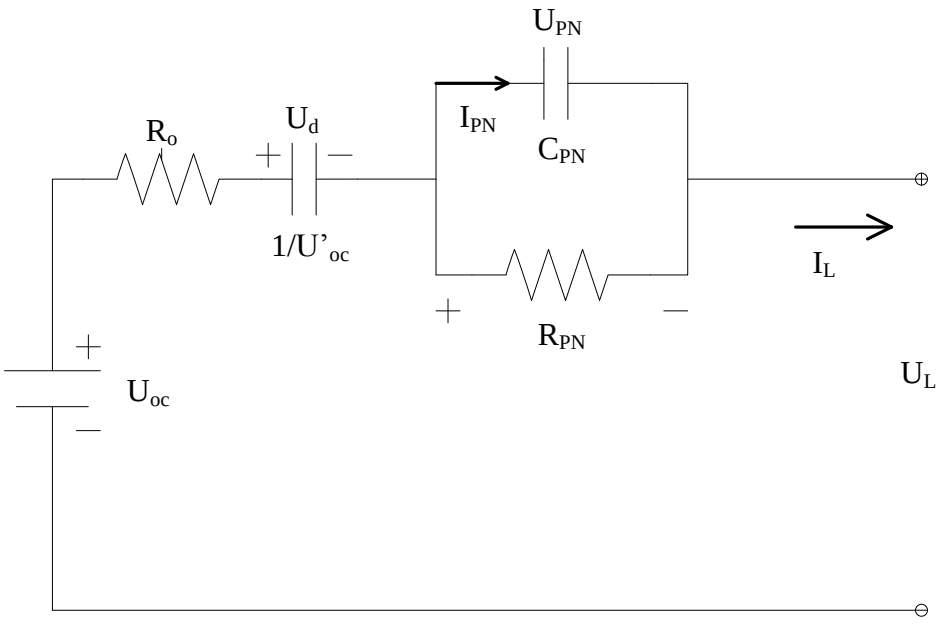

Figure 7. Schematic diagram of the PNGV battery model [5].

$$\begin{cases} U_d = U_{oc} I_L \\ U_{PN} = -\dfrac{U_{PN}}{R_{PN} C_{PN}} + \dfrac{I_L}{C_{PN}} \\ U_L = U_{oc} - U_d - U_{PN} - I_L R_o \end{cases} \tag{29}$$

The PNGV circuit model is an expansion of the Thevenin equivalent circuit model. By adding a capacitor in series with the Thevenin model, PNGV is more accurate at describing the battery performance with a small-current load.

There is another circuit model [20] also built based on the Thevenin equivalent circuit model. In this new circuit model, a nonlinear transfer resistance is used to replace the linear resistance, and the simulation is performed by using MATLAB. A constant current pulse test is used to obtain data for the model pa-

rameters [21]. Then, through a comparison between the new model and the MATLAB lithium-ion model, it shows the new model is more accurate. This model is studied to build a better relationship or to match up the analytical model and circuit model.

The conventional battery circuit model is shown in Fig. 8. $OCV_{(SOC)}$ is a dependent voltage source which is affected by the state of charge (SOC) of the battery. R_i is the battery internal resistance, R_d is linear transfer resistance and C_d is the double layer capacity.

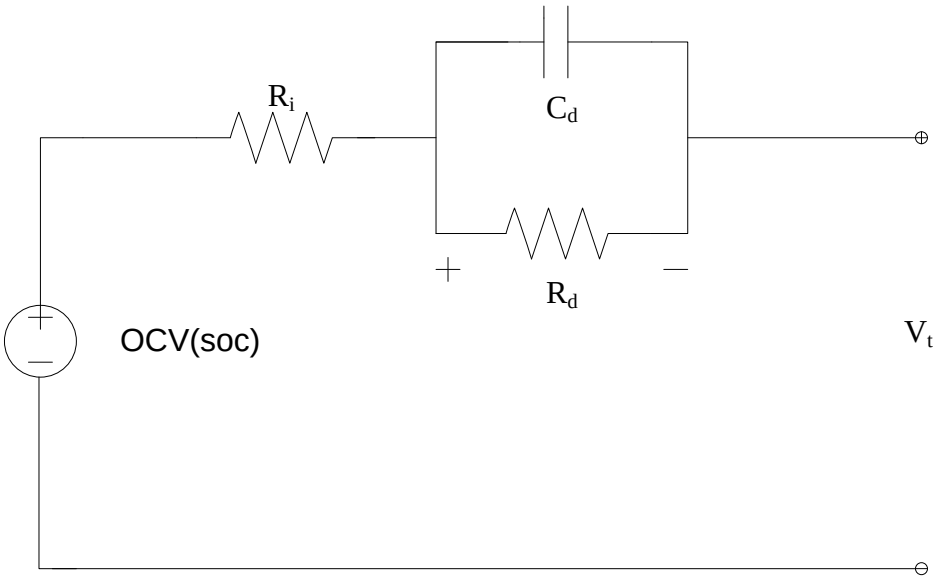

Figure 8. Conventional Thevenin equivalent circuit model of battery.

In the new model shown in Fig. 9, R_i is the internal resistance of the battery which is as same as the conventional circuit model. $R_{d(SOC)}$ is the nonlinear transfer resistance.

To extract the battery model parameters, a controlled current source is controlled by a pulse generator so that the battery will discharge with 1 C for 180 s and then rest for 3420 s. The current pulse test results are found in references [21] and [22]. For this simulation, a 18 Ah Li-ion battery is used, therefore, a constant current of 18 A is discharged to make sure battery discharge with 1 C for 180 s. The current curve is shown in Fig. 10, and the voltage response is shown in Fig. 11.

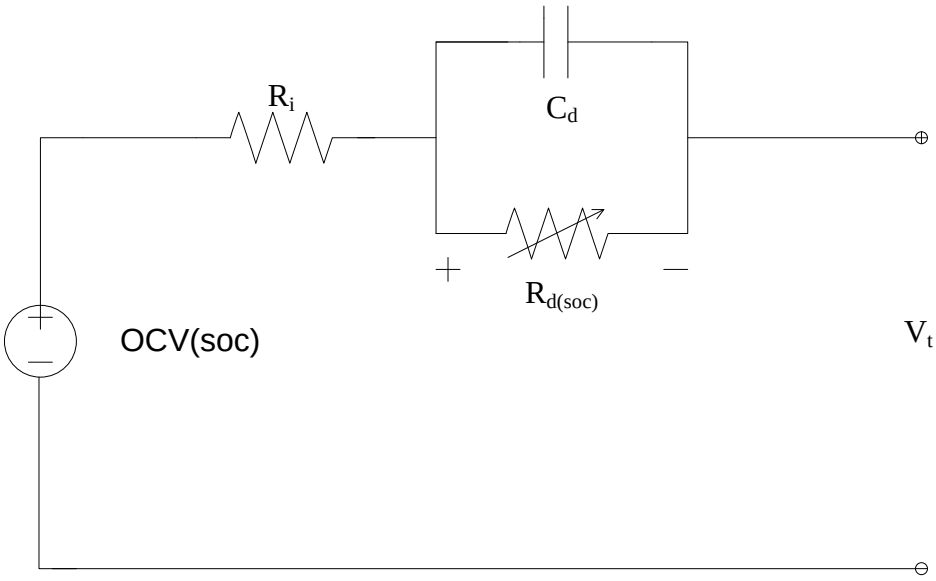

Figure 9. The new battery circuit model with nonlinear transfer resistance.

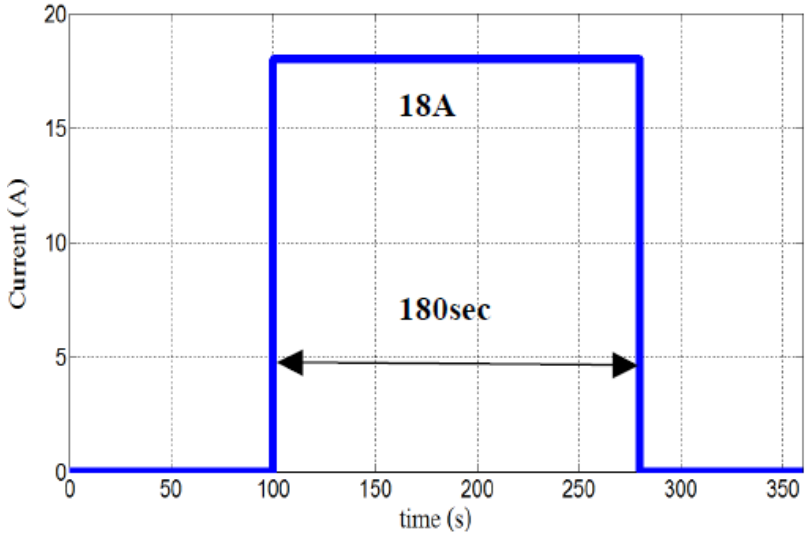

Figure 10. Lithium-ion battery discharges with constant current.

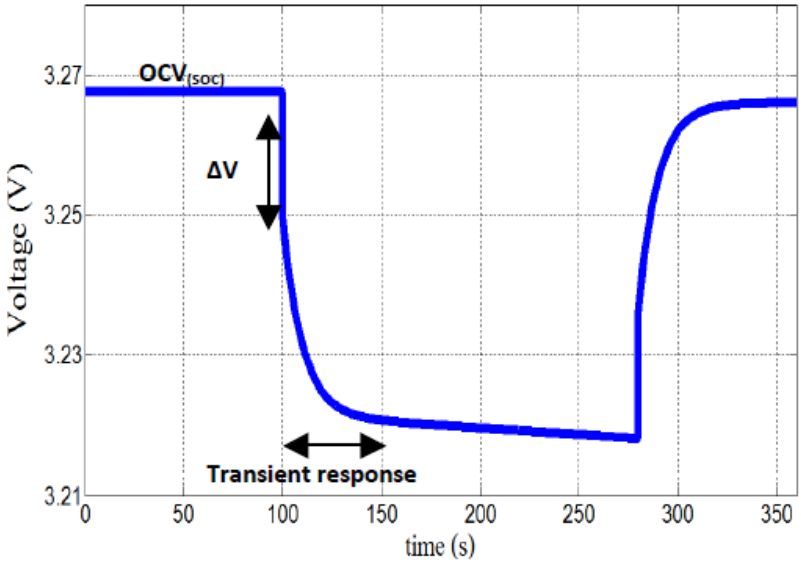

Figure 11. Lithium-ion battery voltage responses with discharge current.

OCV(SOC) is the terminal voltage of battery, the OCV(SOC)-SOC relationship was plotted in Fig. 12. The function of OCV(SOC) was obtained by using a polynomial trend line which fit the curve is shown as:

$$\mathrm{OCV}_{(\mathrm{SOC})} = (3.82 \times 10^{-10})\mathrm{SOC}^5 - (1.21 \times 10^{-7})\mathrm{SOC}^4 + (1.51 \times 10^{-5})\mathrm{SOC}^3$$
$$- (9.3 \times 10^{4})\mathrm{SOC}^2 + 0.03 \times \mathrm{SOC} + 2.85 \qquad (30)$$

From Fig. 12, it shows the open circuit voltage grows fast at the beginning, and after the battery is charged for about 60%, the curve tends to flatten. This appearance also reflects the charging methods which have been shown in Chapter 2. That is charging the battery with a constant current first, then replace the constant current with a constant voltage source and the trickle charge is optional.

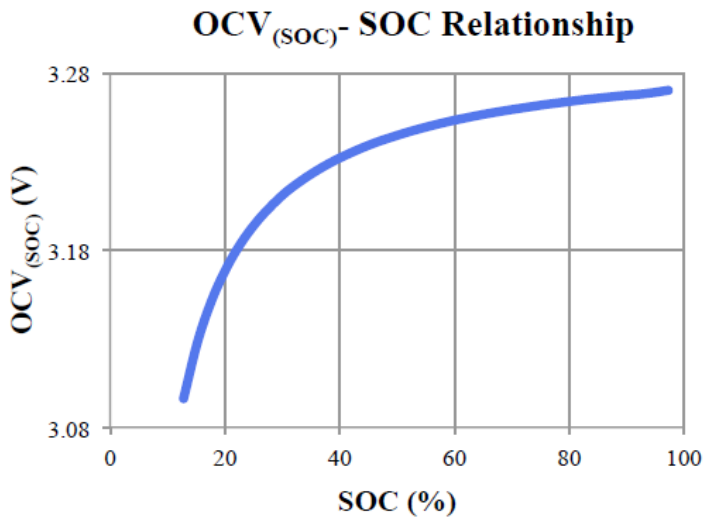

Figure 12. $\mathrm{OCV}_{(\mathrm{SOC})}$-SOC relationship curve.

Another battery model exists in Matlab/Simulink. This model can be used to represent the most popular types of rechargeable batteries, and the equivalent circuit is shown in Figure 13 [24].

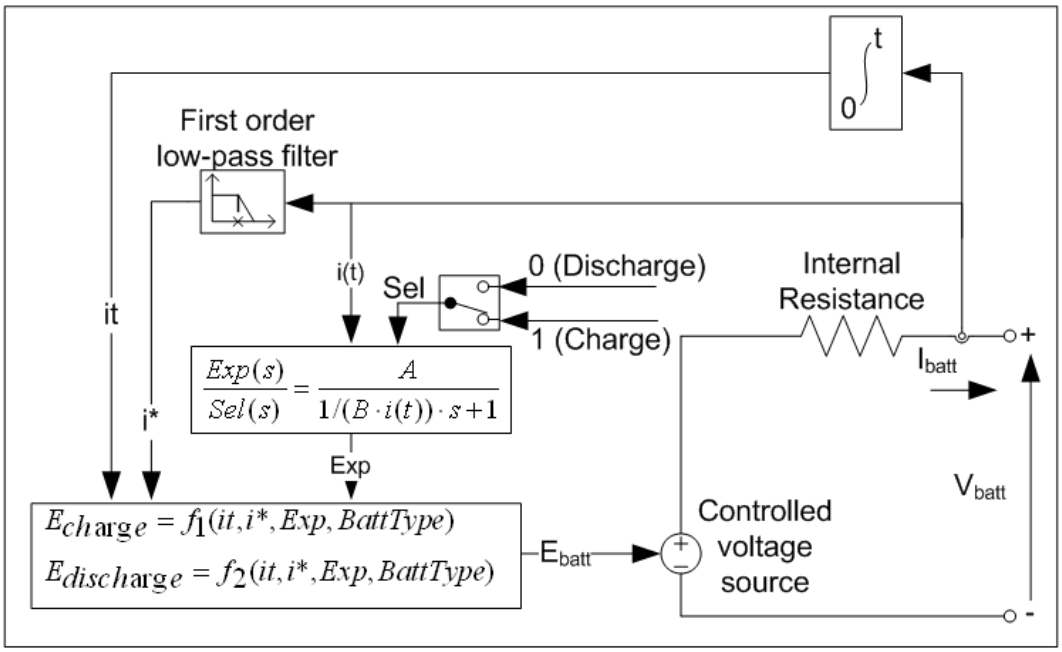

Figure 13. The rechargeable battery equivalent circuit model in Matlab/Simulink.

Where E_{Batt} is the nonlinear voltage (V); E_0 represents the constant voltage (V); *Exp(s)*: the exponential zone dynamics (V); *K*: the polarization constant (Ah^{-1}) or Polarization resistance (Ohms); *i**: the low frequency current dynamics (A); *i*: the battery current (A); i_t is the extracted capacity (Ah); and *Q* is the maximum battery capacity (Ah).

This Matlab/Simulink battery model is available for various types of battery models, so it is convenient to be used as a power source. But this model also has a disadvantage. It makes an assumption that the capacity of the battery does not change with the current amplitude, which also means the battery model will not have a recovery effect during the discharging process. So this leads to a problem that the battery model might be lacking accuracy for battery characteristic analysis.

2.3 Summary

In this chapter, three levels of charging voltage for different chargers have been introduced first. Then, a two-stage charging method with optional trickle charge was studied. In the section on models, two analytical battery models have been shown. The electrochemical diffusion model can describe the battery characteristic precisely but the equations are complicated to calculate. However, the kinetic battery model is simpler and easier to calculate, and also can reflect the battery recovery effect. But the kinetic battery model has a restriction of a constant current flow, this will limit the use of the model. Because in reality, especially for an electrical vehicle, the discharging current is always changing, it is hard to maintain a constant current. This is the one of disadvantages of the kinetic battery model and needs to be improved. While in the section of battery circuit models, different models have been introduced, such as the RC model, the PNGV model and the Thevenin equivalent circuit model. The Thevenin model is the most widely used model, and has been expanded and upgraded for different types of batteries.

CHAPTER 3

BATTERY CAPACITY SIMULATIONS AND CIRCUIT MODEL TESTING

3.1 Discharge Process

The kinetic battery model has been chosen to be the analytical model to which an equivalent circuit model will refer to. Unlike the electrochemical diffusion model that needs lots of complicate calculations, the kinetic battery model is more simple and easy to understand. The kinetic battery model focuses on the battery capacity changes while in charging and discharging processes, so it is more general and can be used for different types of rechargeable batteries, such as lead-acid battery and lithium-ion battery. In this chapter a new equation is derived. The new equation can be used for variable discharging or charging current. So the new equation can be applied in different realistic scenarios. For example, if an electrical car is suddenly accelerating, the discharging current will change with respect to the acceleration speed, so the current is not a constant value but a nonlinear curve. In this case, the new equation can be employed to simulate this situation. There is also another example to show where to use the new equation. When people are charging a battery and want to change the normal charge to fast charge which means the current is not a constant value too, the new equation can show the battery capacity with respect to time for both charging and discharging processes with different currents, and show the result to the user.

From reference [8], the author made an assumption that the system will discharge under a constant rate. However, in reality, the discharge current for a power system might change with respect to time. Often it is hard to maintain a constant

discharge rate. So a more general expression to apply to a variable current is needed to represent both the discharge and charging processes of the system.

The idea to obtain the general equation is to replace the constant current with non-constant current in the original differential equations of Equations (14) and (15). Then apply Laplace transform and convolution theory to calculate the q_1 which is the battery capacity.

$$\frac{dq_1}{dt} = kcq_2 - k(1-c)q_1 - I(t) \quad (0 < q_1 \leq cq_{max}) \tag{31}$$

$$\frac{dq_2}{dt} = k(1-c)q_1 - kcq_2 \quad (0 < q_2 \leq (1-c)q_{max}) \tag{32}$$

Applying the Laplace transform to the expressions above, then the equations can be written as follows:

$$sQ_1(s) - q_{1,0} = kcQ_2(s) - k(1-c)Q_1(s) - I(s) \tag{33}$$

$$sQ_2(s) - q_{2,0} = k(1-c)Q_1(s) - kcQ_2(s) \tag{34}$$

Combine and simplify the equations above,

$$Q_2(s) = \frac{q_{2,0} + k(1-c)Q_1(s)}{s + kc} \tag{35}$$

$$Q_1(S) = \frac{kcq_0}{s(s+k)} + \frac{q_{1,0}}{s+k} - \frac{s+kc}{s(s+k)}I(s) \tag{36}$$

Using the inverse Laplace transform and convolution theory, then q_1 can be calculated as follows:

$$q_1 = cq_0 - \int_0^t (c - (c-1)e^{-k\tau}) * I(t-\tau) * d\tau \tag{37}$$

This is an extension of the expression of Equation (19), since the constant current is replaced by an arbitrary current waveform.

From Reference [8], the researcher assumed that the discharging process is under a constant current, from which Equation 19 was obtained. Using Equation (19) and assuming that the discharge current is 20 A for the entire process, the discharging process is graphed in Figure 14. Then, the discharge current is changed to 50 A, the plot shown in Figure 15,

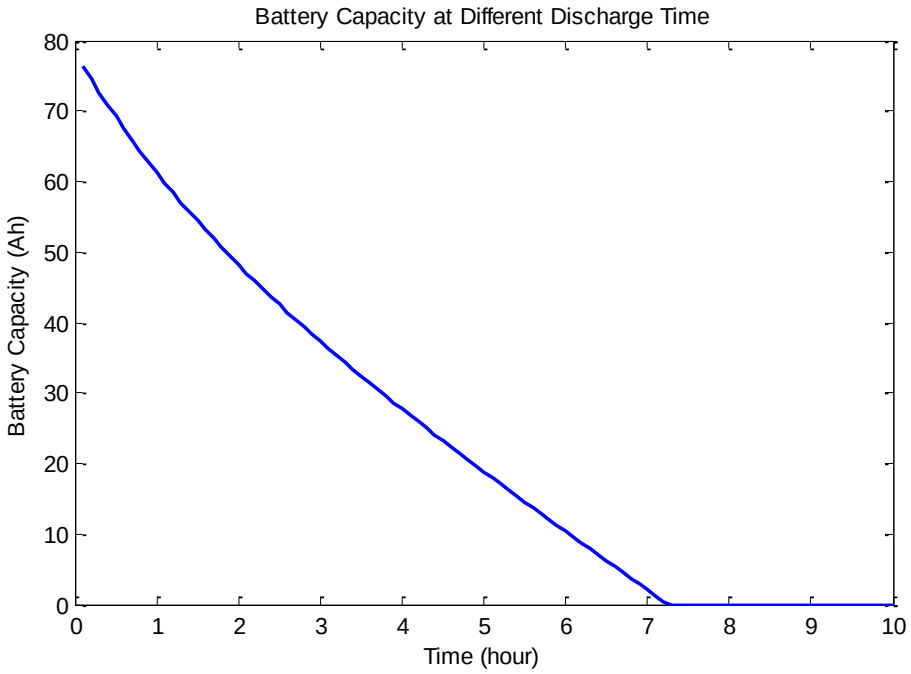

Figure 14. Discharging process under 20 A constant current.

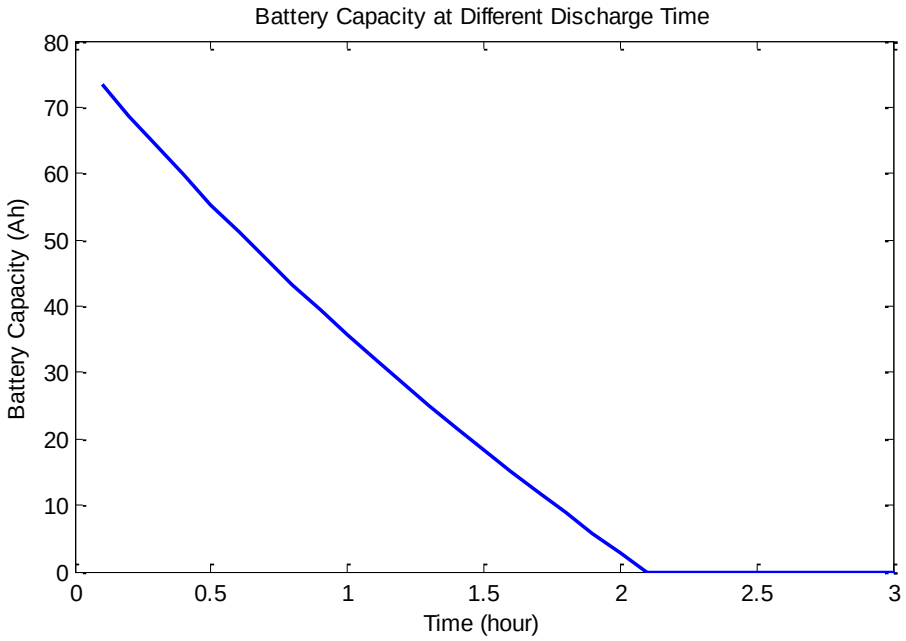

Figure 15. Discharging process with 50 A discharge current.

From a comparison of the two different discharge currents, the graphs show the battery will last longer while applying a lower discharge rate. This can be used in the electrical car battery monitor. For example, when people are driving on the highway and turn on the cruise control, the load of the motor can be assumed to be a constant value, so the battery will be discharged by a constant current. With the Equation (19), it is easy to evaluate the remaining capacity in the rechargeable battery and tell the driver how long the car can run under this condition. However, in reality, cars always need to accelerate and decelerate, the load of the motor will change with respect to different speeds.

Equation (37) is obtained for non-constant current which can be used in all conditions. Here we assume the car will undergo a uniform acceleration motion

after running at constant speed, which means the discharge current of the battery will increase. For convenience sake using convolution theory, Equation (37) is rewritten as follows over three separate distinct time periods,

$$q_1 = cq_0 - \int_0^{t1} [(1-c)e^{-k\tau} + c] * I(t-\tau)d\tau - \int_{t1}^{t2} [(1-c)e^{-k\tau} + c] * I(t-\tau)d\tau - \int_{t2}^{t} [(1-c)e^{-k\tau} + c] * I(t-\tau)d\tau \quad (38)$$

A three step current plot has been drawn in Fig. 16, the current starts at 15 A and then jumps to 30 A, which can represent the uniformly accelerating process. The current drops back to 15A at the last time period which starts at hour 5.

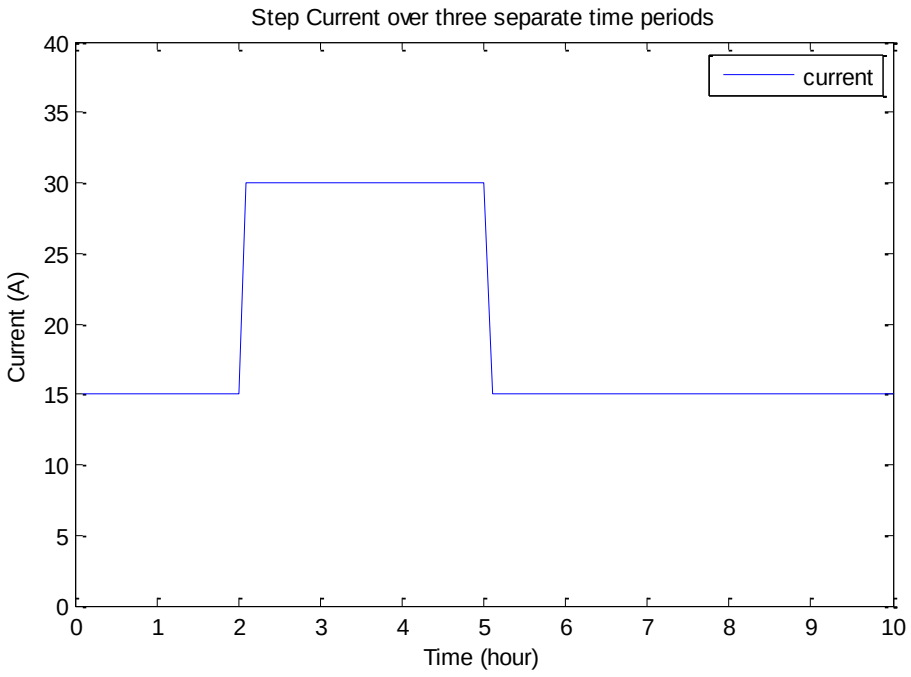

Figure 16. Three current steps versus time.

The three current steps are filled into Equation (38) and the battery response is plotted in Fig. 17. The falling slope of the curve indicates the car is accelerating.

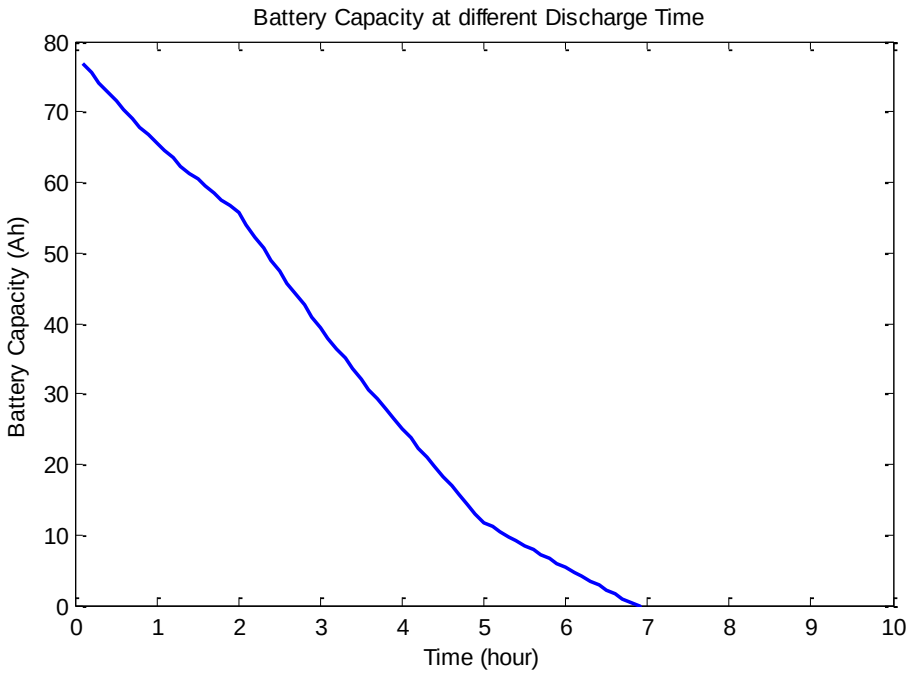

Figure 17. Discharge process with three different current steps.

An analytical method is used here to prove Equation (38) is correct. First, separate the total discharge time into three periods from 0 hr to 2 hr, 2 hr to 5 hr and 5 hr to 10 hr. For the first time period, substitute the current value into Equation (37), and the function can be simplified as

$$q_{1,1} = 79.576 + 15.42(e^{-0.5821t} - 1) - 6.025t \quad (0 \le t \le 2\ hr) \qquad (39)$$

Then calculate the charge at time 2 hr, $q_{1,1}$ = 69.34 Ah. Substitute this value and the second time period into Equation (37). The function for the second period is

$$q_{1,2} = 72.24 + 30.84 * e^{-0.5821t} - 12.048t \quad (2 \le t \le 5\ hr) \qquad (40)$$

Calculate the charge at time equals 5 hr, $q_{1,2}$ = 13.68 Ah, then fill in the function again with the calculated value and third period current, the final expression is

$$q_{1,3} = 42.96 + 15.42 * e^{-kt} - 6.02t \quad (5 \leq t \leq 10) \tag{41}$$

The plot of the three expressions is drawn in Figure 18.

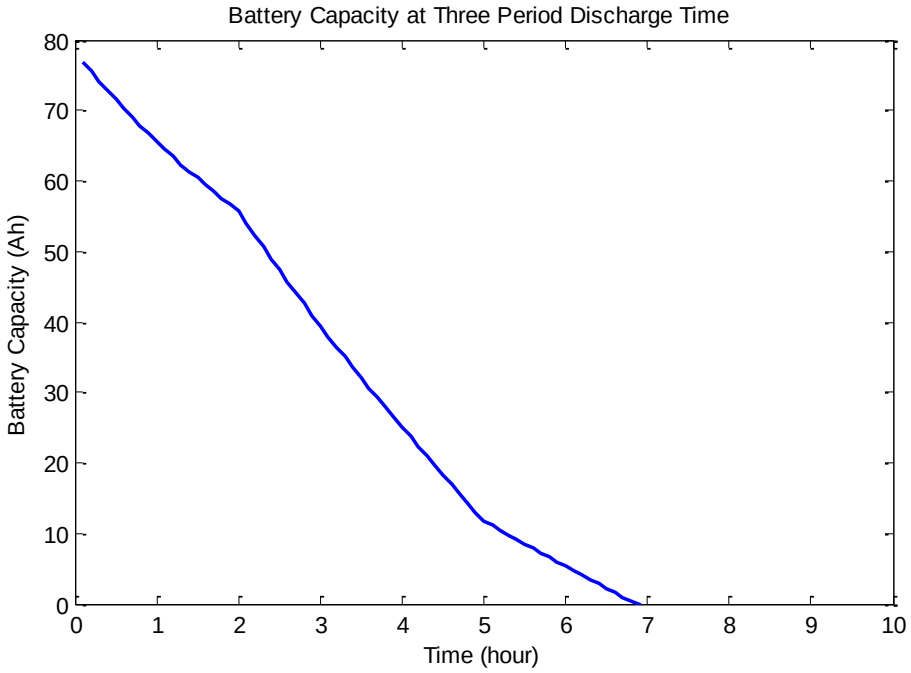

Figure 18. Analytical method with three period discharge time.

Comparing Fig. 17 with Fig. 18 shows that the two results are identical, which means the analytical method proves the theory for the variable current is correct. The graph itself also makes physical sense. When the current increases, the battery discharges faster than while at a lower discharge rate, and when the current turned back to the original rate, the slope of the curve also changed back. The battery capacity curve can help people to know the performance of the bat-

tery. This also can help to predict the remaining energy in the battery, and provide an easily understandable signal to the user. For example, in Fig. 18, the second time period is from 2 hr to 5 hr with discharge rate of 30 A. If the plot in this period represents a machine performing an uniform acceleration, it is not hard to anticipate that the battery can only support the machine to keep accelerating like this for another 0.93 hr, then the battery capacity would reach zero. However, the machine will not keep accelerating after 5 hr, and begin to move at a constant speed. Instead, the current changes back to 15 A, then from Fig. 18, the final discharge time is 6.95 hr. In reality, it is very important to estimate the battery capacity for the electrical vehicle. There is a customer report from Nissan, that the power indicator showed the battery having 17 miles left before needing charge, however, the car only ran for about 5 miles, then it shut down on the road. The expression of Equation (38) can also be used on an electrical vehicle, the battery capacity can be estimate correctly and the remaining energy can be predicted and shown to the driver.

From Fig. 18, the falling slope of the curve indicates the car is accelerating. And the output current was comprised of abrupt changes. While in reality, the current may change gradually, so the equation and model also need to be flexible for the situation. This also means the discharge current function can be linear or even nonlinear. Fig. 18 shows the battery capacity performance under a linear discharge current: $I = -3t + 30$ A ($0 \leq t \leq 10$ hr).

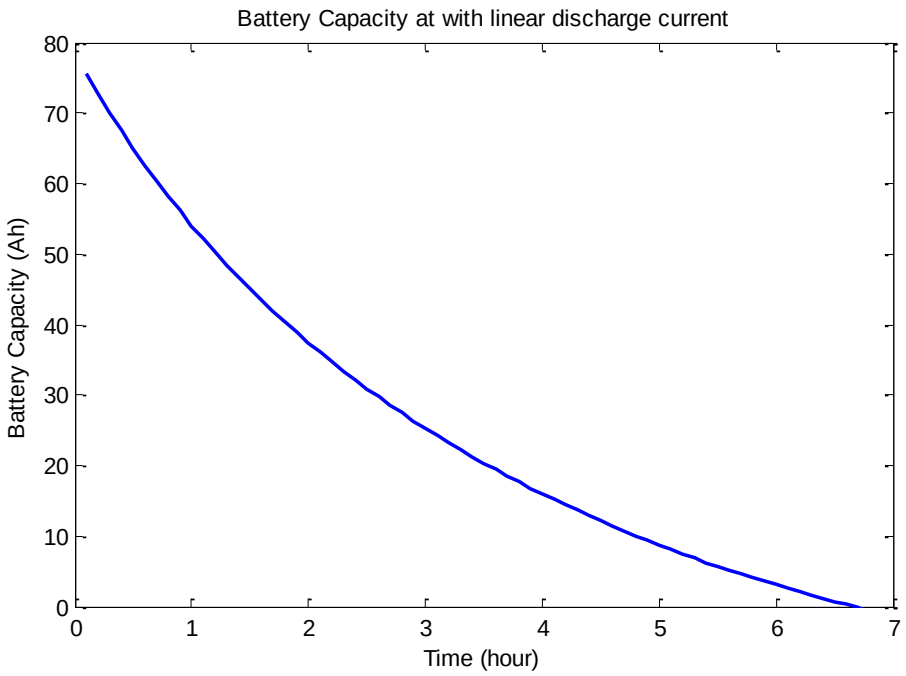

Figure 19. Discharging process with current changing smoothly.

From Fig. 19, it shows the new equations for the kinetic model provide a clear reflection of the discharge process. As can be seen from the curve, the discharge speed at the beginning is fast, and then as the current rate decreases, as well as the reduction of battery voltage, the speed of discharge begin to slow down, and the battery capacity reaches zero at 6.5 hr.

3.2 Charging Process

From the kinetic battery model, it shows the process of how a current flow goes out of the system, and it is under an assumption that the battery capacity is full at the beginning. In general, the charging process is simply the opposite process of discharging. To simplify the calculation, the initial battery capacity is assumed to be zero, and the final condition of the battery capacity is full. Based on

these assumptions, the initial and final conditions are substituted into Equation (19). Rearranging the equation, the constant charging current expression with respect to time can be calculated by the following steps:

Since the charging process is opposite with discharging, the discharging current has been assumed to be positive, so the charging current is assumed to be negative. Then for the charging process, the expression of the capacity in tank one from Equation (19) is now

$$Q_1(s) = \frac{q_{1,0}}{s+k} + \frac{I}{s^2+sk} + \frac{kcq_0}{s^2+sk} + \frac{kcI}{s^3+s^2k}$$

Then, inverse Laplace transforming the expression above, the solution is almost identical to that presented in Equation (19). The equation for the charging process is

$$q_1 = q_{1,0}e^{-kt} - \frac{(q_0kc+I)(1-e^{-kt})}{k} + \frac{Ic(kt-1+e^{-kt})}{k} \qquad (42)$$

Where $q_{1,0} = cq_{\max}$, and $q_0 = q_{1,0}+q_{2,0}$. The equation above can be simplified as

$$q_1 = q_0 \cdot c + \frac{I(1-e^{-kt})(1-c)}{k} + Ict$$

Assume the battery final charge is $q_1 = cq_{\max}$, then the maximum current to fully charge the battery can be expressed as

$$I_c = \frac{-kcq_{max} + kq_{1,0}e^{-kt} + q_0kc(1-e^{-kt})}{1-e^{-kt}+c(kt-1+e^{-kt})} \qquad (q_0 \geq 0) \qquad (43)$$

Incorporating Equation (43) into Matlab, then Fig. 19 can be simulated as shown in Fig.20.

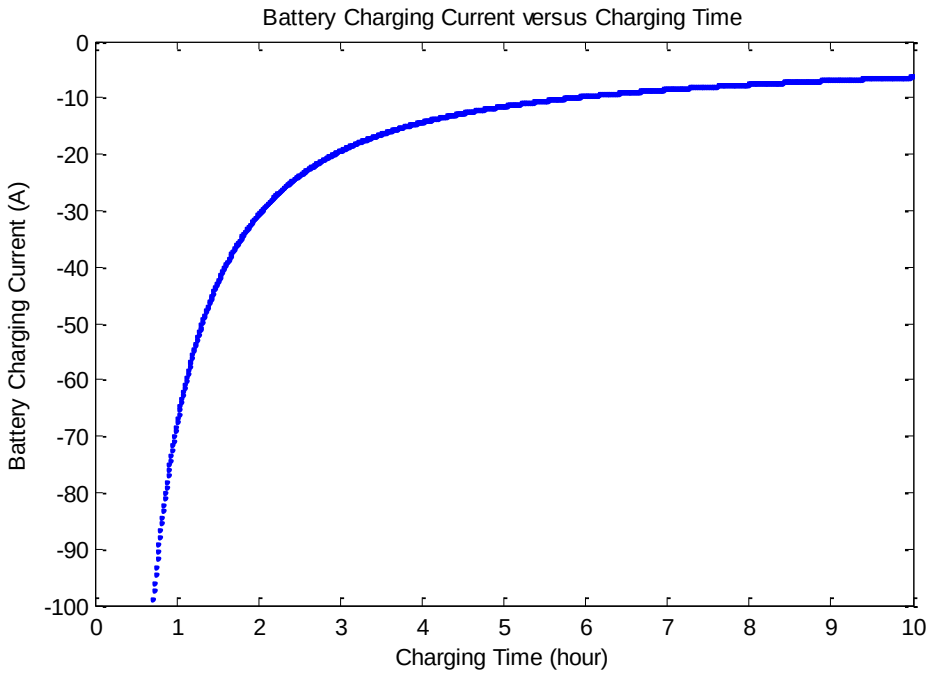

Figure 20. Battery charging current versus charging time.

In Fig. 20, the Y axis means the amount of constant charging current during one full charging process, and the X axis means the charging time during the process. Namely, in the plot it shows the battery will be fully charged at 1 hour with 78 A charging current, and it will takes 2 hours to fully charge the battery at about 32 A.

It is known that the charging process is an opposite of the discharging process, so the general charging function for various charging currents can be obtained by substituting different initial and final conditions into Equation (38).

$$q_{charging} = 0 - \int_0^t [(c-1)e^{-k\tau} - c] * I(t-\tau)d\tau \qquad (44)$$

Assuming the charging current is 20 A, and inputing the value into Equation (44), then a plot of the battery capacity performance during the charging process is drawn in Fig. 21. This plot shows the behavior of the battery charging process under a constant 20 A current by using the improved kinetic model function.

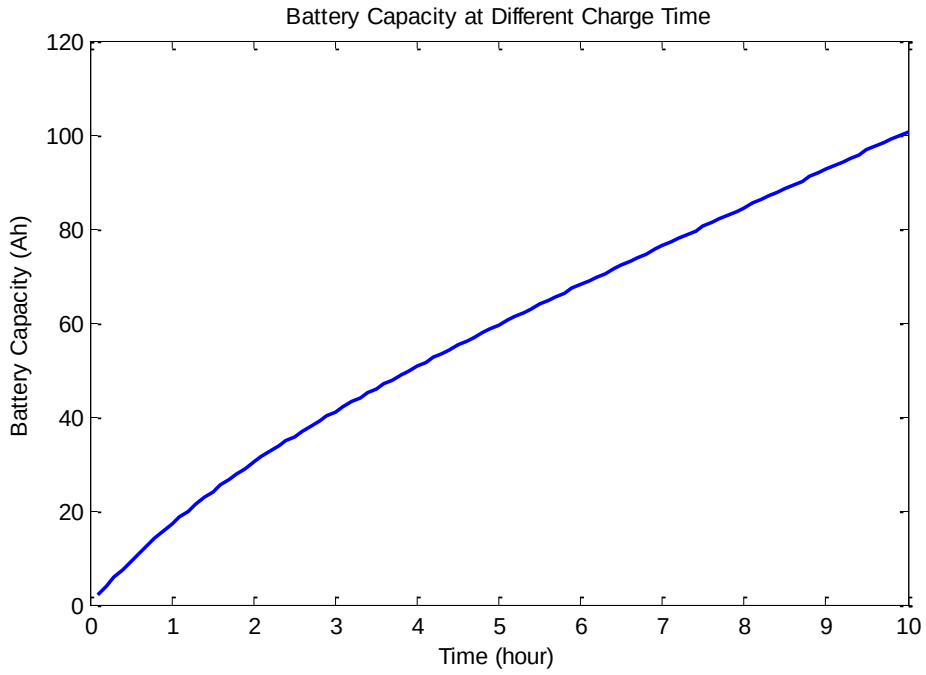

Figure 21. Charging process with 20 A current.

To further develop Equation (44), substitute the constant current to a function of a linear current (or nonlinear current). The piecewise-integrator method has been employed to expand Equation (44) and make the new charging equation more general like previous sections which have shown in the discharging process. The three periods charging current has been applied here again. Fig. 22 shows the battery capacity performance with three different charging currents (15, 30 and 15 A).

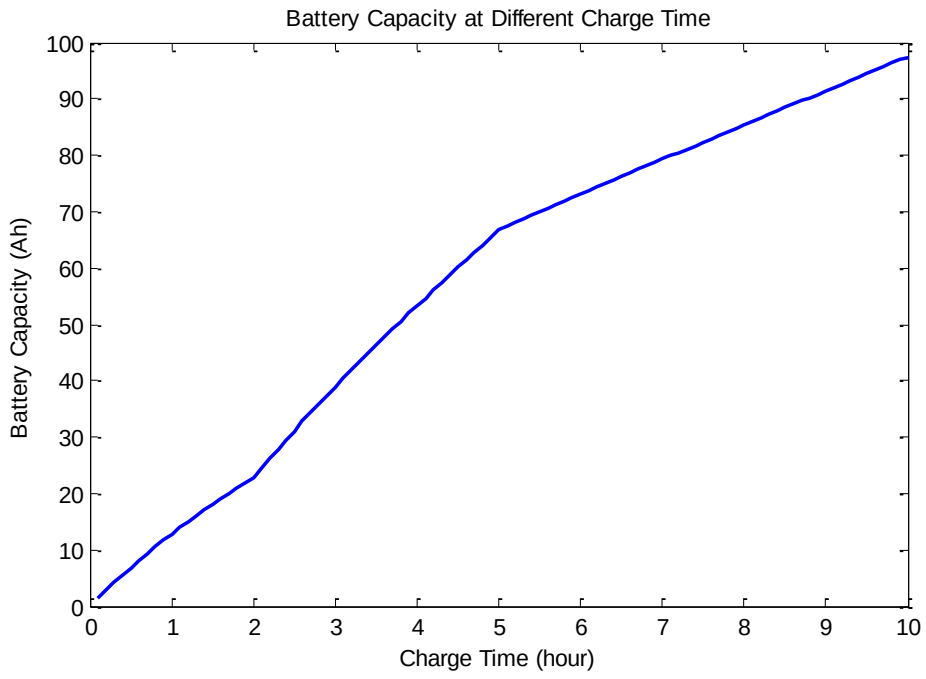

Figure 22. Charging process with three different steps current.

Fig. 22 shows the battery is charged by three different current steps. The current plot has been shown in Fig. 16. As can be seen from Fig. 22, when a higher charging current flows into the battery, the battery charge will increases significantly faster than the lower current process.

After using the three different current steps, instead, we change the step current into a linear current with a function of $I = -3t + 30$ A ($0 \leq t \leq 10$ hr). With a continuously decreasing current, the battery charging curve will become smoother than the process with step currents. Fig. 23 shows the curve tends to be flat when the battery is approaching to fully charged.

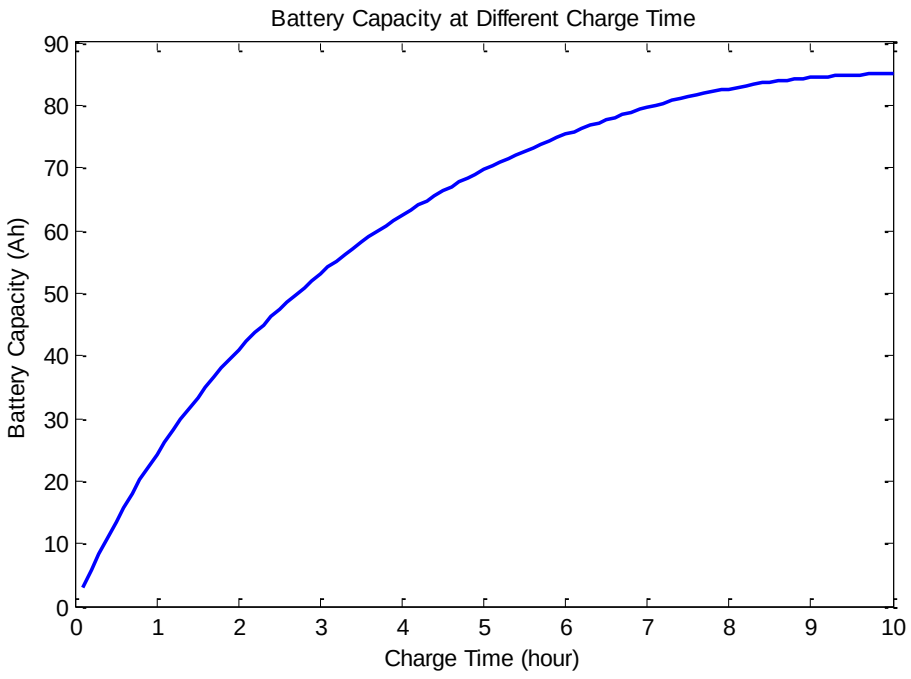

Figure 23. The charging process with the current changing smoothly.

3.3 The New Circuit Model

The Kinetic Battery model is an intuitive model, which was developed from a chemical model. And it is actually a first-order approximate expression for the diffusion model. However, to simulate the battery characteristics, like the *I*-*V* relation in computer electrical software, a circuit model, see Fig. 24, which matches with the kinetic battery model is needed. In this section, using time domain nodal analysis, a circuit model which has analogous differential equations with the kinetic battery model has been obtained.

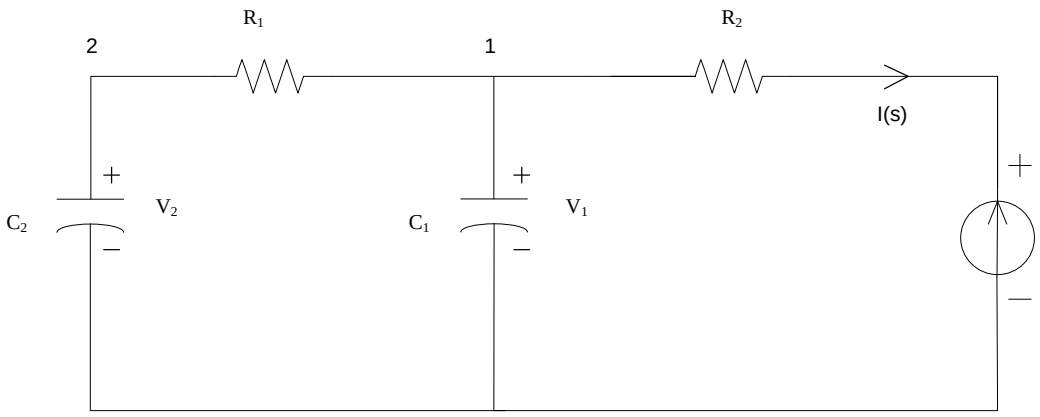

Figure 24. The circuit model for the kinetic battery model.

In Fig. 24, C_1 and C_2 are two capacitors of the battery, R_1 is the restriction resistor between the two capacitors, and R_2 is the battery internal resistor. Focusing on point 1 and point 2, nodal analysis is performed and two differential equations can be written as

$$0 = C_2 \frac{dV_2}{dt} + C_1 \frac{dV_1}{dt} + I(t) \tag{45}$$

$$\frac{V_1 - V_2}{R_1} = C_2 \frac{dV_2}{dt} \tag{46}$$

Where V_1 and V_2 are the voltages of their two capacitors and $I(t)$ is the output current.

While in the charging process, the voltage initial condition for the two capacitors is zero, which means $V_1(0) = V_2(0) = 0$. Combining Equations (45) and (46), permits re-writing Equation (45) as

$$C_1 \frac{dV_1}{dt} = \frac{V_2}{R_1} - \frac{V_1}{R_1} - I(t) \tag{47}$$

$$C_2 \frac{dV_2}{dt} = \frac{V_1 - V_2}{R_1} \tag{48}$$

By comparing Equations (31) and (32) with above two expressions, the relationships between different parameters in both the circuit model and kinetic model are found.

Using Laplace transform on the differential equations of the circuit model, the two functions can be written as a matrix,

$$\begin{bmatrix} \frac{1}{R_1} & -sC_2 - \frac{1}{R_1} \\ sC_1 + \frac{1}{R_1} & -\frac{1}{R_1} \end{bmatrix} \begin{bmatrix} V_1(s) \\ V_2(s) \end{bmatrix} = \begin{bmatrix} 0 \\ -\frac{I}{s} \end{bmatrix}$$

After solving the matrix, the two expressions of $V_1(s)$ and $V_2(s)$ can be acquired.

$$V_1(s) = \frac{-I(sR_1C_2 + 1)}{s^2(sC_1C_2R_1 + C_2 + C_1)}$$

$$V_2(s) = \frac{-I}{s^2(sC_1C_2R_1 + C_2 + C_1)}$$

It is known that for capacitors, $Q = CV$, so multiply $V_1(s)$ and $V_2(s)$ by their own capacitance, and compare the new expressions with the Laplace transform of Equations (19) and (20). The relationships between parameters are

$$k = \frac{C_1 + C_2}{R_1C_1C_2} \tag{49}$$

$$c = \frac{C_1}{C_1 + C_2} \tag{50}$$

The same expression can also be obtained by calculating the circuit impedance which has been shown in Fig. 25.

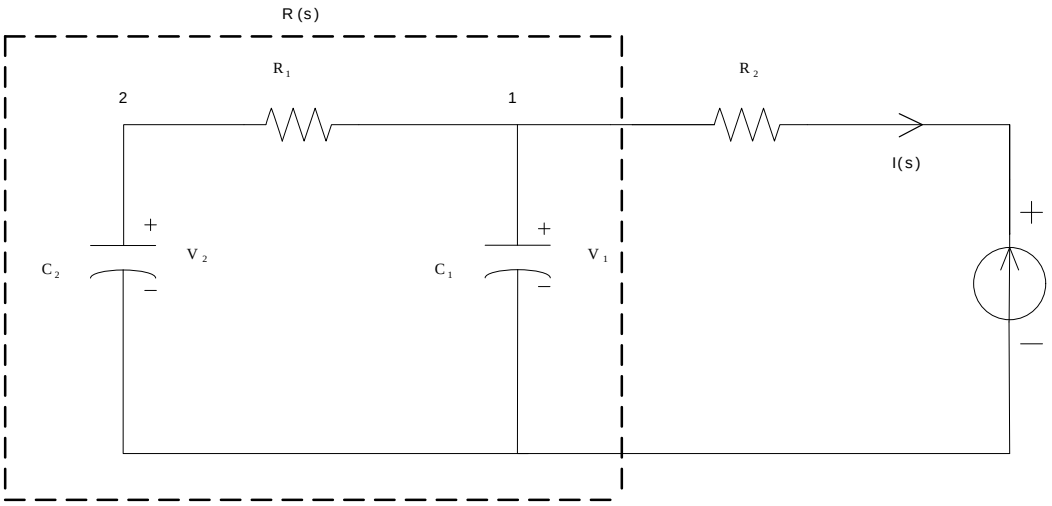

Figure 25. The impedance of C_1, C_2, and R_1.

$R(s)$ is the total impedance of C_1, C_2, and R_1 as shown in Fig. 24, and $R(s)$ can be calculated as

$$R(s) = \frac{1 + sR_1C_2}{sC_1 + R_1s^2C_1C_2 + sC_2}$$

In the discharging process, the current has been assumed to be positive. Then, for the charging process, the current is negative. According to $V = RI$, the voltage of $R(s)$ is obtained.

$$V_1(s) = \frac{1 + sR_1C_2}{sC_1 + R_1s^2C_1C_2 + sC_2} \cdot (-I(s))$$

Then, the instantaneous charge of the battery can be calculated by using $Q_1 = C_1V_1$,

$$Q_1(s) = \frac{s + \frac{1}{R_1C_2}}{s\left(s + \frac{C_1 + C_2}{R_1C_1C_2}\right)} \cdot I(s)$$

For the analytical model, assume the initial charge of the capacitors is zero. The charging process expression of the analytical model can be simplified as

$$Q_1(s) = \frac{s + kc}{s(s + k)} \cdot I(s)$$

Since the circuit model is built based on the analytical model results, the two expressions should match each other. Comparing those two equations together, then the same relationship as shown in Equation (49) and (50) for C_1, C_2, R_1 and k can be obtained.

3.3.1 Matlab Simulation

The circuit diagram in Matlab/Simulink has been drawn in Fig. 26. The voltmeter is used to monitor the voltage of C_1, and a step current is used to provide a constant 20 A current during the charging process. It is necessary to calculate the value of the electronic components before running the simulation. The parameter values can be calculated by using Equations (49) and (50).

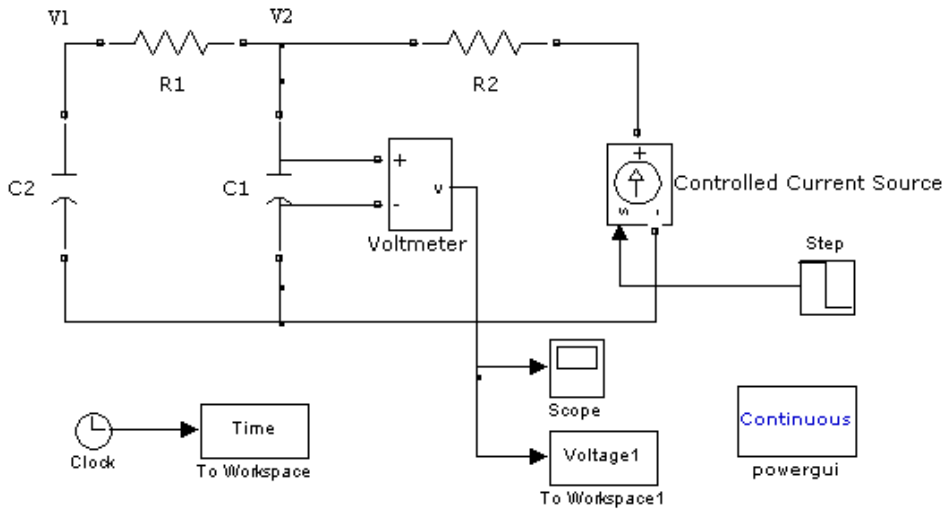

Figure 26. Matlab/Simulink circuit model for the kinetic battery model.

According to the kinetic model, it is known that k = 0.58, and c = 0.401. The battery has a total capacity (both tank 1 and tank 2 are included) of 196 Ah, which means for tank 1 (the instantaneous battery capacity) capacity can be calculated as

$$q_1 = c \cdot q_{max} = 78.4\ Ah$$

While the battery is fully charged, the voltage of the battery is 11.5 V, and the capacity of C_1 can be achieved.

$$C_1 = \frac{q_1}{V_1} = \frac{78.4\ Ah \times 3600\ s}{11.5\ V} = 24542\ F$$

Substitute the values for c, k and C_1 into Equations (49) and (50), then the parameters are calculated and shown in Table 1.

TABLE 1. Parameter values for circuit model

Parameter	c	k	C_1	C_2	R_1	R_2	q_1
Value	0.401	0.58	24542 F	36813 F	0.421 Ω	0.0013 Ω	78 Ah

Inserting these values into Matlab/Simulink, a plot of the capacitor 1 voltage is shown in Fig. 27.

As is known for capacitors, $Q = CV$, so multiply $V_1(s)$ by its own capacitance, and comparing the data with the kinetic model, a new plot is shown in Figure 27.

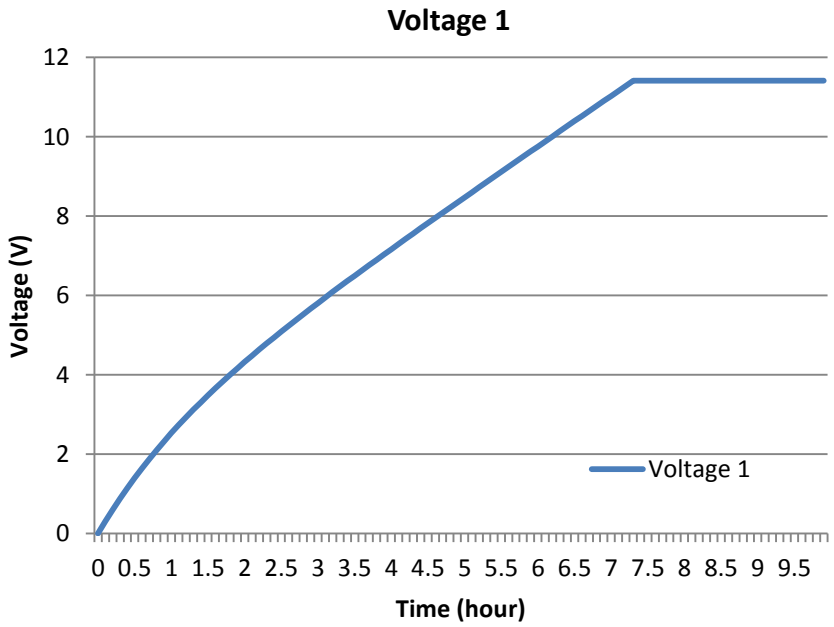

Figure 27. The voltage curve of Capacitor 1.

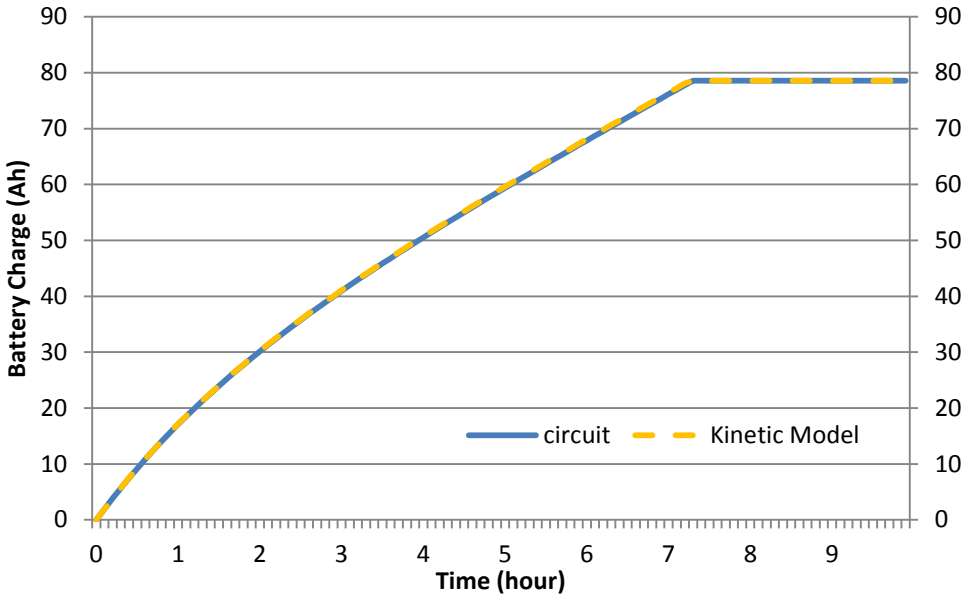

Figure 28. Comparison of battery rate capacity between the circuit model and kinetic model.

As can be observed from Fig. 28, the two curves of the kinetic model and the circuit model are almost matched. To be more precisely, the root-means-square deviation is calculated as following.

$$R = \frac{\sqrt{\sum(y_1 - y_2)^2}}{Number\ of\ data} \tag{51}$$

Where y_1 and y_2 are the data of the two battery capacity curves, and R is the root-means-square deviation, the value of R is 0.014 Ah (0.02% of the maximum capacity). This value is small enough and demonstrates an ideal circuit model based on the kinetic model has been built. The circuit model can be used in various simulation tools, such as Matlab/Simulink, PSpice and Plecs. The PSpice simulation software will be employed in the following section to demonstrate this capability.

3.3.2 PSpice Model

In Fig. 29, a piecewise linear current source (IPWL) is used to provide power to charge the two capacitors. Table 2 shows the parameter properties for the current source. Comparing with the Matlab circuit diagram, the PSpice circuit has an added resistor, R_3. R_3 is set with large resistance (10^5 Ω), and serves to keep the circuit from having a floating node error. In this section, a constant 20 A current is used to charge the two capacitors. However, as shown in Table 2, the initial current of the current source is zero. From T_1, it shows the current abruptly changes to 20 A from 0 A at 0.0001 s. This is because the IPWL current source does not have a zero initial condition, so an initial time interval from 0 s to t^{++} is needed to establish a zero initial condition, and the smaller the time interval from 0 A to 20 A is, the more accurate the result will be. So the t^{++} is assumed to be as small as possible. Here in Table 2, the t^{++} which is also set to be T_2 has the chosen value, 0.0001 s. Fig. 30 shows the plot of the Capacitor 1 voltage with constant 20 A charging current. The rms deviation (R) in this simulation is 0.048 Ah (0.06% of the maximum capacity).

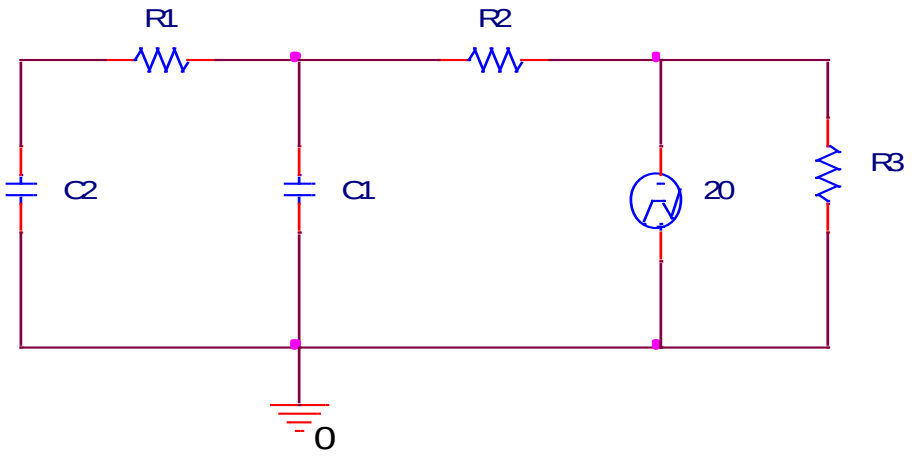

Figure 29. PSpice circuit model diagram.

Table 2. Parameter properties for the IPWL current source

Parameter	I_1	I_2	I_3	T_1	T_2	T_3
Value	0 A	20 A	20 A	0 s	0.0001 s	36000 s

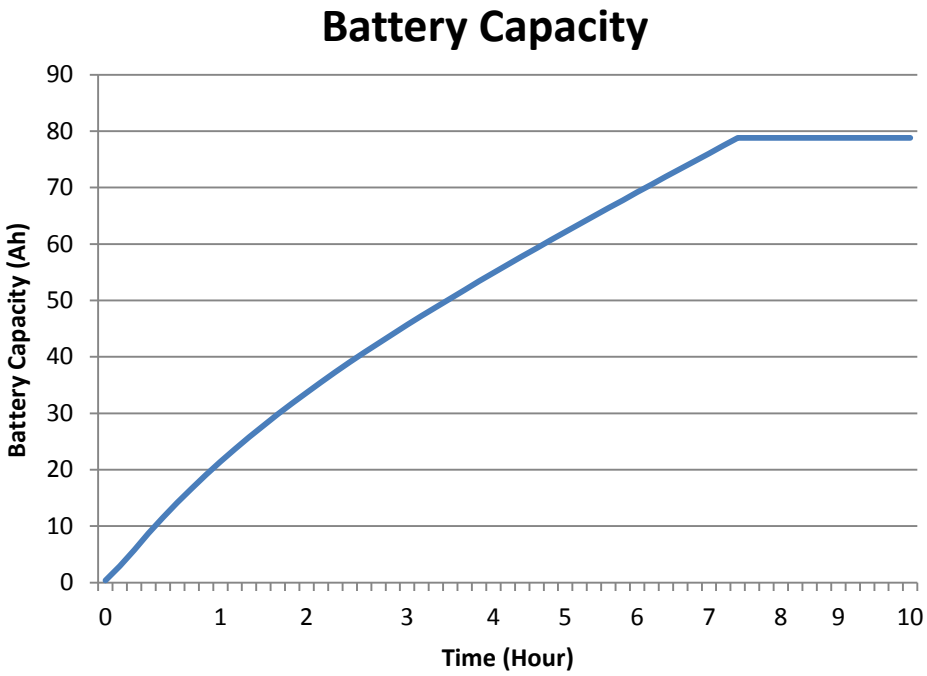

Figure 30. Voltage of Capacitor 1 in charging process.

The curve in Fig. 30 is similar to that in Fig. 28 which is the result for the prior simulation with Matlab/Simulink. The circuit model is proved deployable for multiple simulation software, but the circuit model also needs minor adjustment for different simulation tools.

3.4 Battery Realistic Charging Process Simulation

In this section, a two-stage charging method is used to simulate a realistic charging process. The first stage is charging the battery with constant current, and the battery will be charged to its voltage. Then, the second stage will keep charging the battery with constant rate voltage until the battery is fully charged. From the International Standard – IEC 60898-1 [23], for a garage circuit breaker, the

commonly-available preferred values for the rated current are 6 A, 10 A, 13 A, 16 A, 20 A, 25 A, 32 A, 40 A, 50 A, 63 A, 80 A, 100 A and 125A.

Since the 20 A constant current has been used for previous simulations, for convenience, the current for the circuit breaker in the garage is assumed to be 20 A. Then, this two-stage simulation was performed in Matlab/Simulink. In the first stage, the constant 20 A current is employed to charge the battery, and the circuit diagram is the same as the Fig. 26. The circuit charged for 7 hours and 43 minutes with constant current. At that point, Capacitor 1 has been charged to 11.5 V, meaning the battery has reached its rated voltage. However, Capacitor 2 has not been fully charged yet. At the end of the first stage, the total charge for the two capacitors is 145 Ah, and this is 74% of the battery total charge.

In the second stage, a constant voltage source with 12.5 V replaced the current source. The reason to choose a 12.5 V source is considering the energy lost from the battery internal resistance, R_2. In the second stage, Capacitor 2 will keep charging to 11.5 V. The new circuit diagram is shown in Fig. 31. The second stage lasted 7 hours and 15 minutes until the battery was fully charged. This simulation depicts a real battery charging process with an adjustable charger, and the simulation parameters can be altered to match the requirements for different rechargeable batteries. Table 3 shows the parameters and results of this two-stage charging process. The combination of the two stages is presented in Fig. 32.

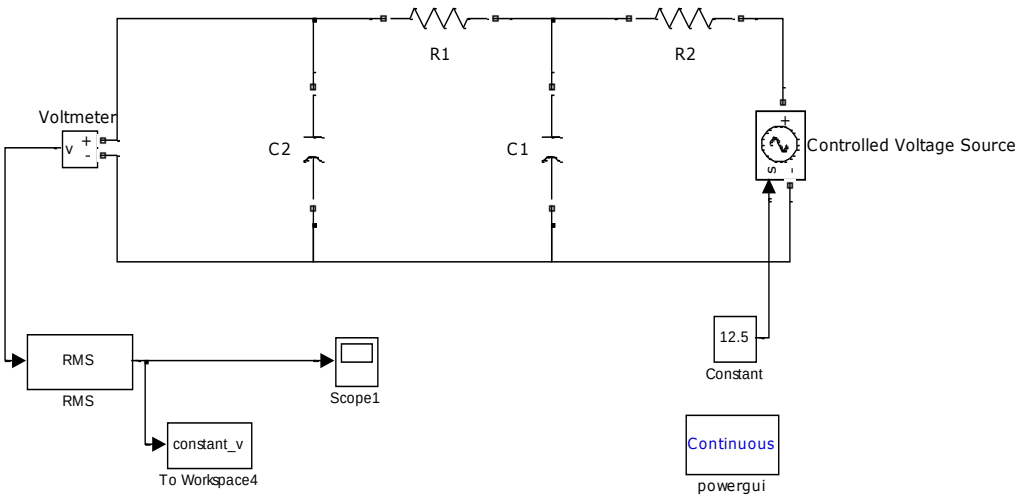

Figure 31. Battery charging process with constant voltage.

Table 3. Parameters and results for the two-stage charging process

Stages	*I*	*V*	Charging Time	Final Capacity
Constant Current	20 A	Various	7.73 hrs	145 Ah
Constant Voltage	Various	12.5 V	7.26 hrs	196 Ah

From this two-stage battery charging process, the real performance for a battery in the charging process has been simulated. As can be seen from Fig. 32, the slope of the curve means the battery charging speed. The battery has a faster charging speed under a constant charging current rather than a constant charging voltage. Here in this example, the circuit breaker is assumed to have a 20 A rated current,

while if a higher rated circuit breaker is allowed, the charging time will be shorter. In fact, a garage charger using Level 1 charging would be hard pressed to completely charge a car battery overnight.

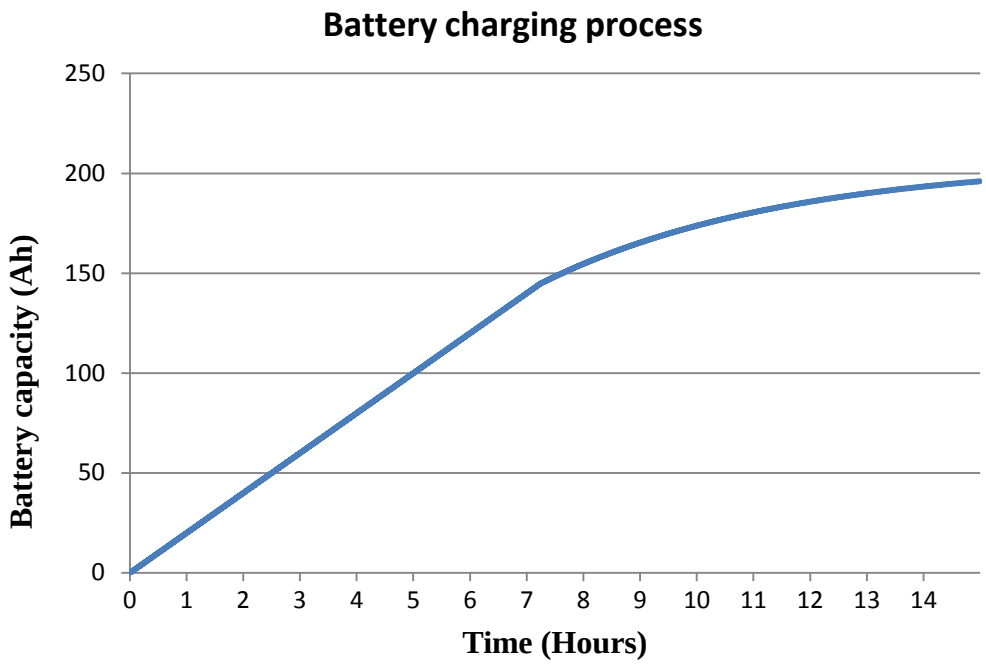

Figure 32. The two-stage battery charging process.

CHAPTER 4

CONCLUSIONS AND FUTURE WORK

4.1 Main Conclusions

In this thesis, the history and the importance of the rechargeable battery have been introduced, and different battery models are studied, such as the electrochemical diffusion model, the kinetic battery model and several circuit models. At the same time, an issue of finding the relationship between an analytical battery and the circuit model is posed. This relationship is a key point to implement the analytical model into the computer simulation tools, and it also plays an important role in better understanding the battery characteristics.

In Chapter 3, the kinetic battery model is chosen to be the analytical model, which is also the reference for the new circuit model. The analytical battery model has been implemented in Matlab/ Simulink for a six-cell battery using a 196 Ah, 12.5 V lead-acid battery. From the study of the kinetic battery model, new equations for both discharging and charging processes are derived. The new equations allow the kinetic battery model to describe an arbitrary nonlinear capacity variation of the battery while in various operating conditions. In Section 4.1, the original constant current is replaced by a linear reducing discharge current. From the battery capacity curve, it shows the battery discharges fast at the beginning, then, as the current flow decreases, the discharging process slows down. This also makes the kinetic battery model more useful in realistic scenarios.

After further work, a new circuit model has been obtained based on the kinetic battery model. Since the circuit model is built on the analytical model, the relationship between the two models has been found. The Matlab/Simulink and PSpice simulation tools have been employed to test the accuracy of the new circuit model. By comparing the plots of the circuit model and the kinetic battery model together, and by calculating the root-mean-square deviation for the two curves, the value is 0.014 Ah, which prove the accuracy of the circuit model in reference to the kinetic battery model. This also means the relationship between the analytical model and the circuit model is reliable.

At last, a realistic battery charging process is simulated by the new circuit model, to show how the circuit model can represent charging by a garage charger. In Chapter 2, the charging method used by a typical charger was introduced. In Section 4.4, the new circuit model is first charged by a constant current, then charging continues until fully charged under a constant voltage. The plot in Fig. 31 shows the battery capacity performance with the two-stage charging method. Comparing Fig. 32 with Fig. 2, the shape of the battery capacity curves for both graphs are similar. This shows the new circuit model can be used to correctly simulate the battery charging process by a normal charger.

4.2 Future Works

The future work will be concentrated on the following aspects.

1. To better improve the accuracy of the new circuit model, a feedback control system can be added to the circuit. Considering in reality, the batteries

usually have a recovery effect, which means the unavailable charge of the battery will become available after a period with no or a low current. So, if a feedback control system can be applied on the battery to simulate the recovery effect, this will upgrade the circuit model.

2. Comparing the circuit model of the kinetic battery model with the Thevenin equivalent circuit model, the two same current functions will be applied to both of the models, and calculate the root-mean-square deviation between the data of the two models. Finally, assess the accuracy of which model more closely describes the battery realistic performance.
3. The electrochemical diffusion model will continue to be studied, and the partial differential equations of the electrochemical model can be solved by ordinary differential equations. Then extract the values that are useful to build a circuit model based on the electrochemical diffusion model, and compare the electrochemical circuit model with the kinetic battery circuit model. Since the electrochemical model is the most accurate analytical model to describe the battery characteristics, so the electrochemical circuit model is suppose to be more accurate than the kinetic circuit model.
4. The rechargeable battery lifetime issue might be considered. The simulation could not only focus on a single charging or discharging cycle, but also can estimate the lifetime cycles and provide a relationship between the battery capacity and battery life cycles.

REFERENCES

[1] Mehdi Erezadi-Amoli, K.Choma, *"Rapid-Charge Electric-Vehicle Stations," IEEE Transactions on Power Delivery*, vol. 25, no. 3, July 2010, pp 1883-1886.

[2] V. Pop, H J Bergveld "State-of-the-art of battery state-of-charge determination," *Meas. Sci. Technol*. 16 (2005) R93-R110.

[3] M. Winter, R. J.Brodd, "What are Batteries, Fuel Cells, and Supercapacitors?" *Chem. Rev*.104, 4245 (2004); D. A. Scherson, A. Palencsar, Electrochem. Soc. Interface 15, 17 (2006).

[4] M. Doyle, T.F. Fuller, and J. Newman, "Modeling of galvano-static charge and discharge of the lithium/polymer/insertion cell," *J. Electrochem.* Soc., vol. 141, no. 1, pp. 1-9, Jan. 1994.

[5] Hongwen He, Rui Xiong and Jinxin Fan, "Evaluation of Lithium-Ion Battery Equivalent Circuit Models for State of Charge Estimation by an Experimental Approach", *Energies*, ISSN: 1996-1073, vol. 4, no. 582, 2011 .

[6] Mark Verbrugge, Edward Tate, "Adaptive state of charge algorithm for nickel metal hydride batteries including hysteresis phenomena," *Journal of Power Sources* 126 (2004) 236-249.

[7] Kandler A. Smith, Christopher D. Rahn, Chao-Yang Wang, "Control oriented 1D electrochemical model of lithium ion battery," *Energy Conversion and Management* 48 (2007) pp: 2565-2578 .

[8] J. Manwell and J. McGowan, "Lead acid battery storage model for hybrid energy systems," *Solar Energy*, vol. 50, pp. 399–405, 1993.

[9] M. R. Jongerden and B. R. Haverkort, "Which battery model to use*?," IET Softw,*. vol. 3, no. 6, pp. 445-457, Dec. 2009.

[10] "Motor Trend 2004 Car of the Year Winner: Toyota Prius". MotorTrend Magazine. Source Interlink Media. Retrieved on 2008-05-30.

[11] Kevin Morrow, Donald Karner, "Final report of Plug-in hybrid electric vehicle charging infrastructure review", U.S. Department of Energy Vehicle Technologies Program-Advanced Vehicle Testing Activity, Contract No.58517, November 2008.

[12] J. F. Manwell, J. G. McGowan, "Evaluation of Battery Model for Wind/Hybrid Power System Simulations", *J.5th European Wind Energy Association*, pp. 1182-1187, October 1994.

[13] A.G. Ritchie "Recent developments and future prospects for lithium rechargeable batteries" *J.Power Sources*., vol. 96, no. 1, pp. 1-4, June. 2001.

[14] Isidor Buchmann, Batteries in a Portable World. Third edition. Publisher: Cadex Electronics Inc. Apr, 2011.

[15] Min Chen, G. A. Rincon-Mora, "Accurate, Compact, and Power-Efficient Li-Ion Battery Charger Circuit", *IEEE Transactions on Circuits and Systems II: Express Briefs*, vol: 53, Issue: 11, 2006, pp. 1180 – 1184.

[16] Domenico D. D and Giovanni F, "Lithium-Ion battery State of Charge estimation with a Kalman Filter based on a electrochemical model". *IEEE International Conferences on Control Applications*, pp 702-707, 2008.

[17] Kiehne, H.A, Battery Technology Handbook 2003, 2nd ed., Publisher: New York : M. Dekker, 2003, 515 p. page 17, Figure 1.8.

[18] V.H. Johnson, "Battery performance models in ADVISOR", *Elsevier Journal of Power Sources*, vol.110, Issue 2, pp.321-329, 22 August. 2002.

[19] PNGV Battery Test Manual, Revision 3, U.S. Department of Energy. Assistant Secretary for Energy Efficiency and Renewable Energy, Idaho Operations Office, Feb 2001.

[20] Low Wen Yao, Aziz, J.A., "Modeling of Lithium Ion battery with nonlinear transfer resistance", *IEEE Applied Power Electronics Colloquium (IAPEC)*, pp. 104 – 109, April 2011.

[21] S.J Lee et.al, "State-of-Charge and Capacity estimation of Lithium-ion Battery Using New Open-Circuit Voltage versus State-of-Charge*," Journal of Power Sources*, 185 (2008), pp. 1367-1373, 2008.

[22] S. Bernhard et al."Modeling of High Power Automotive Batteries by the Use of an Automated Test System,"*IEEE Transactions on Instrumentation and Measurement*, vol 52, no. 4, pp 1087-1091, August 2003.

[23] "Electrical Accessories - Circuit-Breakers for Overcurrent Protection for Household and Similar Installations - Part 1: Circuit-Breakers for A.C. Operation." *International Electrotechnical Commission* 60898-1, July, 2003

[24] Tremblay, O, Dessaint, L. A. "Experimental Validation of a Battery Dynamic Model for EV Applications." *World Electric Vehicle Journal*. vol. 3 - ISSN 2032-6653 - © 2009 AVERE, EVS24 Stavanger, Norway, May 13 - 16, 2009.

[25] Taesic Kim, Wei Qiao, "A Hybrid Battery Model Capable of Capturing Dynamic Circuit Characteristics and Nonlinear Capacity Effects", *IEEE Transactions on Energy Conversion*, vol. 26, no. 4, December 2011, pp. 1172-1180.

[26] P.T Moseley, "Research results from the Advanced Lead-Acid Battery Consortium point the way to longer life and higher specific energy for lead/acid electric-vehicle batteries," *J. Power Source*, vol 73, issue 1, 1998, pp. 122-126.

[27] Aurelien Du Pasquier, Irene Plitz, "A Comparative Study of Li-ion Battery, Supercapacitor and Nonaqueous Asymmetric Hybrid Device for Automotive Applications", *J. Power Source*, 115 (2003), pp. 171-178.

[28] V.Rao, G. Singhal, A.Kumar, and N. Navet, "Battery modeling for embedded systems," *in Proc.18thInt. Conf. VLSI Design*, 2005, pp. 105-110.

[29] C. Chiasserini and R. Rao, "A model for battery pulsed discharge with recovery effect," *in Proc. Wireless Commum. Netw. Conf.*, 1999, pp. 636-639.

[30] M. Chen and G.A.Rincon-Mora, "Accurate electrical battery model capable of predicting runtime and I-V performance," *IEEE Trans. Energy Convers*, vol. 21, no. 2, pp. 504-511, Jun. 2006.

APPENDIX A

MATLAB CODE FOR KINETIC BATTERY MODEL

The code of using the new kinetic battery model equations.

```
clc
clear
syms T;
time = 0.1:0.1:10;
time = time';

c = 0.4;
k = 0.58;
% vector initialization
current = zeros(length(time),1);
q1f = zeros(length(time),1);
q1b = zeros(length(time),1);
q1c = zeros(length(time),1);
q1d = zeros(length(time),1);
q1e = zeros(length(time),1);

% for i=1:length(time)
%    t=time(i);
%    if i>=1 && i<=20
%        current(i) = 15;
%         q1f(i)=79.576+20.41*(exp(-0.5821*t)-1)-8.12*t;
%     elseif i>=21 && i<=50
%        current(i) =30;
%        q1f(i)=73.98+51*exp(-k.*t)-20.3*t;
%    else
%        current(i)=15;
%        q1f(i)=14.748+20.41*exp(-k.*t)-8.12*t;
%    end
% end
for i=1:length(time)
    t=time(i);
    current(i) = 30-3*t;
end

figure(10)
plot(time,current(i),'b')
```

```
title('Step Current over three separate time periods')
xlabel('Time (hour)');
ylabel('Current (A)');
legend('current')
q1a = c*196-20*(1-exp(-k.*time))./k+c*20*(1-exp(-
k.*time))./k-c*20*time;
for i=1:length(time)
    t=time(i);
if q1a(i)<=0
  q1a(i)=0;
else
  q1a(i)=q1a(i);
end
end
%figure (1)
total = c*196;
total2 = total;
total3 = 0;
total4 = 0;
for i=1:length(time)
    t=time(i);
    q1b(i)=c*196+int(((c-1)*exp(-k.*(t-T))-
c)*(current(i)),T,0,t);%one step
    q1c(i)=c*196+int(((c-1)*exp(-k.*T)-
c)*(current(i)),T,0,t);%I(t-T)
   % term1 = int(((c-1)*exp(-k.*t)-c)*(20),T,0,t-0.1);
   % term2 = int(((c-1)*exp(-k.*t)-c)*(20),T,t-0.1,t);
    increment = int(((c-1)*exp(-k.*(t-T))-
c)*(current(i)),T,t-0.1,t);
    total = total + double(increment);
    q1d(i) = total;  % this one does not obtain the
correct answer
    increment = int(((c-1)*exp(-k.*T)-
c)*(current(i)),T,t-0.1,t);
    total2 = total2 + double(increment);
    q1e(i) = total2;
    increment2 = int(((c-1)*exp(-k.*T)-
c)*(current(i)),T,t-0.1,t);
    total3 = total3 - double(increment2);
    q2e(i)=total3;
    increment3 = int(((c-1)*exp(-k.*T)-c)*(20),T,t-
0.1,t);
    total4 = total4 - double(increment3);
    q2f(i)=total4;
end
figure(1)
```

```
plot(time,q1a,'b');
title('Battery Capacity at Different Discharge Time')
xlabel('Time (hour)');
ylabel('Battery Capacity (Ah)');
legend('q1a')
figure(2)
plot(time,q1b,'g--');
title('Battery Capacity at Different Discharge Time')
xlabel('Discharge Time (hour)');
ylabel('Battery Capacity (Ah)');
legend('q1b (one-step with I(T))')
figure(3)
plot(time,q1c,'r-.');
title('Battery Capacity at Different Discharge Time')
xlabel('Discharge Time (hour)');
ylabel('Battery Capacity (Ah)');
legend('q1c (one-step with I(t-T))')
figure(4)
plot(time,q1d,'m--');
title('Battery Capacity at Different Discharge Time')
xlabel('Discharge Time (hour)');
ylabel('Battery Capacity (Ah)');
legend('q1d (increment with I(T))')
figure(5)
plot(time,q1e,'k:');
title('Battery Capacity at Three Period Discharge Time
')
xlabel('Time (hour)');
ylabel('Battery Capacity (Ah)');
%legend('q1e (increment with I(t-T))')
figure(6)
plot(time,q1f,'b--');
title('Battery Capacity at Different Discharge Time')
xlabel('Discharge Time (hour)');
ylabel('Battery Capacity (Ah)');
legend('q1f (three step method)')
figure(7)
plot(time,q2e,'g');
title('Battery Capacity at Different Charge Time')
xlabel('charge Time (hour)');
ylabel('Battery Capacity (Ah)');
legend('q2e(charging process with different current)')
figure(8)
plot(time,q2f,'b');
title('Battery Capacity at Different Charge Time')
xlabel('Time (hour)');
```

```
ylabel('Battery Capacity (Ah)');
legend('q2f(charging process with 20 A current)')
```

The code of using the original kinetic battery model equations.

```
clear all
syms c k t1 t2 I1 I2 q1 q2;
 %I1 is the discharge current at 20A
 %I2 is the discharge current at 50A
 %q1 is the battery capacity at 20A discharge current
 %q2 is the battery capacity at 50A discharge current
 %c is the fraction of capacity that may hold availa-
ble charge
 %k is the rate constant
 I1=20;
 I2=50;
 q1=145;
 q2=105;
 t1=q1/I1;
 t2=q2/I2;
 temp1 = 196*c*k/((1-exp(-k*t1))*(1-c)+k*c*t1)-I1;
 temp2 = 196*c*k/((1-exp(-k*t2))*(1-c)+k*c*t2)-I2;

[c0,k0]=solve(temp1,temp2);
 c0=eval(real(c0));
 k0=eval(real(k0));
% syms k c t q Q E E0 Emin
Q=78.6;
%Q is the maximum capacity of the battery
c=c0;
k=k0;
a=1;
% q=zeros(1,11);
figure(1)

for t=0.1:0.1:50
    q(a) = Q*c*k*t/((1-exp(-k*t))*(1-c)+k*c*t);
    plot(t,q(a),'r');
    title('Battery Capacity at Different Discharge
Time')
    xlabel('Discharge Time (hour)');
    ylabel('Battery Capacity (Ah)');
    hold on;
    a=a+1;
end
```

```
figure(2)
Emin=11.5;
E0=12.457;
a=1;
for t=0.1:0.1:50
    E(a)=Emin+(E0-Emin)*q(a)/Q
    plot(t,E(a),'b');
    title('Battery Internal Discharge Voltage at Dif-
ferent Discharge Time')
    xlabel('Discharge Time');
    ylabel('Battery Internal Discharge Voltage');
    hold on;
    a=a+1;
end
figure(3)
a=1
for t=1:0.1:50
    I(a)=196*c*k/((1-exp(-k*t))*(1-c)+k*c*t)
    plot(t,I(a),'r');
    title('Battery Discharge Current versus Discharge
Time')
    xlabel('Discharge Time');
    ylabel('Battery Discharge Current');
    hold on;
    a=a+1;
end
figure(4)
a=1
for t=0.1:0.01:10
    I(a)=(-k*c*196+196*(1-c)*k*c*(1-exp(-k*t)))/(1-
exp(-k*t)+c*(k*t-1+exp(-k*t)))
    plot(t,I(a),'b--');
    title('Battery Charging Current versus Charging
Time')
    xlabel('Charging Time');
    ylabel('Battery Charging Current');
    hold on;
    a=a+1;
end
```

APPENDIX B

SIMULATION DATA FOR THE BATTERY VOLTAGE OF THE CIRCUIT MODEL AND THE KINETIC BATTERY MODEL

Time	V(C1:2)	CIRCUIT	ANALYTICAL	Difference Between Circuit model and Analytical
1.00E-06	8.15E-12	1.959662	1.965838	3.81E-05
1.08E-06	8.89E-12	3.854037	3.86594	0.000142
1.25E-06	1.05E-11	5.686792	5.704023	0.000297
1.59E-06	1.44E-11	7.46139	7.483594	0.000493
2.26E-06	2.49E-11	9.181095	9.207962	0.000722
3.60E-06	5.70E-11	10.84899	10.88025	0.000977
6.29E-06	1.65E-10	12.46799	12.5034	0.001254
1.17E-05	5.59E-10	14.04084	14.08019	0.001549
1.93E-05	1.52E-09	15.57012	15.61325	0.00186
2.99E-05	3.66E-09	17.0583	17.10504	0.002185
4.68E-05	8.94E-09	18.50767	18.55791	0.002524
7.25E-05	2.14E-08	19.92041	19.97404	0.002876
0.0001	4.08E-08	21.29859	21.35553	0.003242
0.000104	4.41E-08	22.64415	22.70432	0.003621
0.000112	5.07E-08	23.95891	24.02227	0.004015
0.000129	6.40E-08	25.2446	25.31112	0.004424
0.000161	9.06E-08	26.50287	26.57252	0.004851

0.000226	1.44E-07	27.73525	27.80801	0.005295
0.000357	2.50E-07	28.94319	29.01907	0.005758
0.000617	4.62E-07	30.12806	30.20708	0.006243
0.001138	8.87E-07	31.29117	31.37333	0.00675
0.00218	1.74E-06	32.43374	32.51906	0.00728
0.004265	3.43E-06	33.55691	33.64543	0.007837
0.008433	6.83E-06	34.66178	34.75354	0.00842
0.016771	1.36E-05	35.74938	35.84441	0.009032
0.033446	2.72E-05	36.82067	36.91903	0.009675
0.066796	5.44E-05	37.87657	37.9783	0.010349
0.133496	0.000109	38.91795	39.02311	0.011058
0.266896	0.000217	39.94562	40.05426	0.011801
0.533696	0.000435	40.96036	41.07253	0.012582
1.067296	0.00087	41.96288	42.07865	0.013401
2.134496	0.001739	42.95388	43.0733	0.01426
4.268896	0.003478	43.934	44.05713	0.015161
8.537696	0.006955	44.90385	45.03076	0.016106
17.0753	0.013904	45.86402	45.99476	0.017095
34.1505	0.027784	46.81503	46.94968	0.01813
68.3009	0.055477	47.75742	47.89602	0.019212
136.6017	0.110591	48.69165	48.83429	0.020344
273.2033	0.0554	49.6182	49.76492	0.021526
546.4065	0.43387	50.53749	50.68835	0.02276
1092.813	0.846284	51.44993	51.605	0.024047

1692.774	1.276432	52.3559	52.51524	0.025389
2292.736	1.684926	53.25577	53.41943	0.026785
2892.698	2.073765	54.14988	54.31793	0.028239
3492.659	2.444762	55.03856	55.21104	0.02975
4092.621	2.799566	55.9221	56.09908	0.031321
4692.582	3.13967	56.8008	56.98233	0.032951
5292.544	3.466433	57.67493	57.86106	0.034643
5892.506	3.781084	58.54475	58.73553	0.036397
6492.467	4.084743	59.4105	59.60598	0.038213
7092.429	4.378425	60.2724	60.47263	0.040094
7692.39	4.663049	61.13068	61.33571	0.042039
8292.352	4.939453	61.98553	62.19541	0.044049
8892.314	5.208395	62.83715	63.05192	0.046127
9492.275	5.470564	63.68572	63.90543	0.048271
10092.24	5.726585	64.53142	64.7561	0.050483
10692.2	5.977026	65.3744	65.6041	0.052763
11292.16	6.222401	66.21481	66.44957	0.055113
11892.12	6.463179	67.0528	67.29266	0.057532
12492.08	6.699784	67.88851	68.13351	0.060021
13092.04	6.9326	68.72207	68.97223	0.062581
13692.01	7.161979	69.55359	69.80895	0.065213
14291.97	7.388237	70.38319	70.64379	0.067916
14891.93	7.611662	71.21097	71.47685	0.070691
15491.89	7.832515	72.03705	72.30823	0.073539

16091.85	8.051035	72.86151	73.13802	0.07646
16691.81	8.267436	73.68445	73.96632	0.079454
17291.78	8.481915	74.50595	74.79321	0.082522
17891.74	8.694648	75.32609	75.61877	0.085663
18491.7	8.905796	76.14495	76.44307	0.088879
19091.66	9.115507	76.9626	77.26619	0.09217
19691.62	9.323912	77.77911	78.08819	0.095535
20291.58	9.531133	78.59454	78.6	2.98E-05
20891.55	9.737277	78.6	78.6	0
21491.51	9.942447	78.6	78.6	0
22091.47	10.14673	78.6	78.6	0
22691.43	10.35021	78.6	78.6	0
23291.39	10.55296	78.6	78.6	0
23891.35	10.75504	78.6	78.6	0
24491.32	10.95653	78.6	78.6	0
25091.28	11.15747	78.6	78.6	0
25691.24	11.35791	78.6	78.6	0
26291.2	11.5579	78.6	78.6	0
26891.16	11.5579	78.6	78.6	0
27491.12	11.5579	78.6	78.6	0
28091.08	11.5579	78.6	78.6	0
28691.05	11.5579	78.6	78.6	0
29291.01	11.5579	78.6	78.6	0
29890.97	11.5579	78.6	78.6	0

30000	11.5579	78.6	78.6	0